

1 **Two years of near real-time chemical composition of**  
2 **submicron aerosols in the region of Paris using an Aerosol**  
3 **Chemical Speciation Monitor (ACSM) and a multi-**  
4 **wavelength Aethalometer.**

5 **J.-E. Petit<sup>1,2,\*</sup>, O. Favez<sup>1</sup>, J. Sciare<sup>2</sup>, V. Crenn<sup>2</sup>, R. Sarda-Estève<sup>2</sup>, N. Bonnaire<sup>2</sup>, G.**  
6 **Močnik<sup>3</sup>, J.-C. Dupont<sup>4</sup>, M. Haeffelin<sup>4</sup>, and E. Leoz-Garziandia<sup>1</sup>**

7 [1] : Institut National de l'Environnement Industriel et des Risques, Verneuil-en-Halatte,  
8 France

9 [2] : Laboratoire des Sciences du Climat et de l'Environnement (CNRS-CEA-UVSQ), CEA  
10 Orme des Merisiers, Gif-sur-Yvette, France

11 [3] : Aerosol d.o.o., Ljubljana, Slovenia

12 [4] : Laboratoire de Météorologie Dynamique, Institut Pierre Simon Laplace, Ecole  
13 Polytechnique, Palaiseau, France

14 \* now at Air Lorraine, 20 rue Pierre Simon Laplace 57000 Metz, France

15 Correspondence to: J.-E. Petit (je.petit@air-lorraine.org)

16  
17 **Abstract**

18 Aerosol Mass Spectrometer (AMS) measurements have been successfully used towards a  
19 better understanding of non-refractory submicron (PM<sub>1</sub>) aerosol chemical properties based on  
20 short-term campaign. The recently developed Aerosol Chemical Speciation Monitor (ACSM)  
21 has been designed to deliver quite similar artefact-free chemical information but for low-cost,  
22 and to perform robust monitoring over long-term period. When deployed in parallel with real-  
23 time Black Carbon (BC) measurements, the combined dataset allows for a quasi-  
24 comprehensive description of the whole PM<sub>1</sub> fraction in near real-time. Here we present a 2-  
25 year long ACSM & BC datasets, between mid-2011 and mid-2013, obtained at the French  
26 atmospheric SIRTA supersite being representative of background PM levels of the region of  
27 Paris. This large dataset shows intense and time limited (few hours) pollution events observed  
28 during wintertime in the region of Paris pointing to local carbonaceous emissions (mainly  
29 combustion sources). A non-parametric wind regression analysis was performed on this 2-  
30 year dataset for the major PM<sub>1</sub> constituents (organic matter, nitrate, sulphate and source  
31 apportioned BC) and ammonia in order to better refine their geographical origins and assess  
32 local/regional/advected contributions which information are mandatory for efficient  
33 mitigation strategies. While ammonium sulphate typically shows a clear advected pattern,  
34 ammonium nitrate partially displays a similar feature, but less expected, it also exhibits a  
35 significant contribution of regional and local emissions. Contribution of regional background  
36 OA is significant in spring and summer while a more pronounced local origin is evidenced

1 during wintertime which pattern is also observed for BC originating from domestic wood  
2 burning. Using time-resolved ACSM and BC information, seasonally differentiated weekly  
3 diurnal profiles of these constituents were investigated and helped to identify the main  
4 parameters controlling their temporal variations (sources, meteorological parameters). Finally,  
5 a careful investigation of all the major pollution episodes observed over the region of Paris  
6 between 2011 and 2013 was performed and classified in terms of chemical composition and  
7 BC-to-sulphate ratio used here as a proxy of the local / regional / advected contribution of  
8 PM. In conclusion, these first 2-year quality-controlled measurements of ACSM clearly  
9 demonstrate their great potential to monitor on a long term basis aerosol sources and their  
10 geographical origin and provide strategic information in near real-time during pollution  
11 episodes. They also support the capacity of the ACSM to be proposed as a robust and credible  
12 alternative to filter-based sampling techniques for long term monitoring strategies.

### 13 1. Introduction

14 The understanding of the formation and fate of atmospheric particulate pollution in urban  
15 areas represents sanitary, scientific, economic, societal and political challenges, greatly  
16 amplified by increasing media coverage of pollution episodes all around the world. Growing  
17 evidences of adverse health effects of atmospheric pollutants (Chow et al., 2006; Pope and  
18 Dockery, 2006; Ramgolam et al., 2009; WHO, 2012) are illustrated by the fact that ambient  
19 air pollution has been characterized as carcinogenic since December 2013 by the International  
20 Agency for Research on Cancer (IARC, 2013). However, the “aerosol cocktail effect”,  
21 directly linked to the complexity of the chemical composition and sources of the particulate  
22 phase, remains poorly understood.

23 In an effort to fill these lacks of knowledge, worldwide coordinated networking activities  
24 (such as Global Atmosphere Watch, European Monitoring and Evaluation Programme,  
25 AErosol RObotic NETwork) have been documenting, since decades, the chemical, physical  
26 and optical properties of aerosol pollution in various environments. At a European level, this  
27 effort is also supported by the Aerosols, Clouds and Traces gases Research InfraStructure  
28 network (ACTRIS) program which aims at pooling high quality data from state-of-the-art  
29 instrumentation such as the Aerosol Chemical Speciation Monitor (ACSM, Aerodyne  
30 Research Inc., Billerica, MA, USA).

31 The ACSM has been recently developed with the aim of robust and easy-to-use near real-time  
32 and artifact-free measurements of the major chemical composition of non-refractory  
33 submicron aerosol (Organic Matter,  $\text{NO}_3^-$ ,  $\text{SO}_4^{2-}$ ,  $\text{NH}_4^+$  and  $\text{Cl}^-$ ) on long-term basis (Ng et al.,  
34 2011). In parallel, a growing interest is also dedicated worldwide for the monitoring of Black  
35 Carbon (BC), considered as an adequate indicator of potential anthropogenic emission having  
36 sanitary impacts (Janssen et al., 2011). In particular, the use of 7-wavelength Aethalometer  
37 (Magee Scientific, USA) allows furthermore for BC source apportionment (Sandradewi et al.,  
38 2008), proven as robust over long term period (Herich et al., 2011). The combination of  
39 measurements from both instruments may thus constitute an efficient and relatively low-cost  
40 tool for the monitoring of submicron aerosol chemistry and a better knowledge of their  
41 phenomenology. Such strategy may be particularly useful to document aerosol sources and

1 their geographical origin in large urban environments such as large urban areas which are  
2 characterized by a complex mixture of gaseous and particulate pollutions. Paris (France) is  
3 one of the largest European megacities and is rather isolated from other major urban  
4 environments. With ~11 million inhabitants, the Paris region accounts for 20% of total French  
5 population distributed over only 2% of its territory, leading to enhanced exposure to various  
6 types of pollution. Moreover, the flat orography of the Paris region favors pollution transport,  
7 making it representative of North-Western Europe aerosol pollution. AIRPARIF, the regional  
8 air quality monitoring network, recently estimated that, since 2007, about 2 million people per  
9 year have been exposed to poor air quality (referring to daily PM<sub>10</sub> concentrations European  
10 limit values; AIRPARIF, 2014) in this region. Over the past 7 years, annual PM<sub>2.5</sub>  
11 concentrations in Paris have remained quite stable although no continuous monitoring of the  
12 chemical composition of the particulate phase is available to investigate any trends in the  
13 major sources of fine aerosols.

14 A recent research program, based on a 1-year (2009-2010) daily filter sampling carried out at  
15 5 various sites (traffic, urban, suburban and regional background; Ghersi et al., 2010), was a  
16 unique opportunity to give insight into the seasonal variations, sources and geographical  
17 origins of aerosol pollution in the region of Paris (Bressi et al., 2013a,b; Petetin et al., 2013).  
18 However, long-term monitoring strategies based on the chemical analysis of aerosols sampled  
19 on filters are subject to various sampling and analytical artifacts (Appel et al., 1984; Turpin et  
20 al., 1994; Pathak et al., 2004; Cheng et al., 2009) and assumptions (OC-to-OM ratio for  
21 instance); they involve laborious laboratory analyses; they cannot capture processes  
22 governing diurnal variations of atmospheric pollutants and fail to provide rapid diagnostics  
23 during pollution events.

24 In this context, Aerosol Mass Spectrometer (AMS) techniques have provided extremely  
25 valuable information of artifact-free real-time chemical composition of submicron aerosols in  
26 urban areas over the past 10 years (Zhang et al., 2004, 2007; Jimenez et al., 2009). In Europe,  
27 OM and ammonium nitrate are generally the two main constituents of PM<sub>1</sub> (Zhang et al.,  
28 2007), showing, however, significant discrepancies during pollution episodes in terms of  
29 chemical composition. Real-time AMS data have improved the understanding of the physical  
30 and chemical (trans)formation pathways of both fractions, through the characterization of  
31 pollution dynamics and source apportionment analyses. Intensive field campaigns involving  
32 AMS measurements were performed during the 2009 summer and 2010 winter seasons in the  
33 frame of the European MEGAPOLI (Megacities: Emissions, urban, regional and Global  
34 Atmospheric POLLution and climate effects, and Integrated tools for assessment and  
35 mitigation) research program. They greatly improved the understanding of the sources and  
36 transformation processes of Paris aerosols, and especially its submicron organic fraction  
37 (Crippa et al., 2013a,b&c; Freutel et al., 2013; Healy et al., 2012; Laborde et al., 2013, Healy  
38 et al., 2013, Zhang et al., 2014). However, AMS techniques cost, size and intensive control  
39 requirements make them impractical for unattended monitoring. Nevertheless, they may still  
40 represent the best strategy to investigate specific trends in aerosol sources, especially in the  
41 context of elevated and stable PM concentrations as observed over the region of Paris during  
42 the past few years. In that perspective, the recently commercialized ACSM may represent an

1 interesting alternative and may ultimately represent the best strategy to deploy for long term  
2 monitoring of submicron aerosol sources and geographical origins.

3 As part of the ACTRIS project, a new in-situ atmospheric station has been implemented in  
4 2011 at a background site of the region of Paris allowing the chemical, physical and optical  
5 characterization of submicron aerosol pollution at a regional scale. The key aim of the present  
6 paper is to describe and discuss one of the first long-term dataset obtained with the ACSM,  
7 offering opportunities for the evaluation of the scientific relevance of a new experimental  
8 strategy for long term monitoring of near real-time chemical composition of PM<sub>1</sub>. Seasonal  
9 trends, wind sector analysis, diurnal variations and pollution episodes retrieved from a 2-year  
10 real-time measurement ACSM and BC datasets are presented and interpreted in order to  
11 refine the origins and parameters controlling the (trans)formation of particulate pollution over  
12 the region of Paris.

13

## 14 **2. Material and methods**

### 15 **2.1 Sampling site and instrumentation**

16 Long-term in-situ observations of the chemical, optical and physical properties of atmospheric  
17 aerosols have been initiated at SIRTA (Site Instrumental de Recherche par Télédétection  
18 Atmosphérique, <http://sirta.ipsl.fr>) since June 2011 within the EU-FP7 ACTRIS program  
19 (Aerosols, Clouds, and Traces gases Research InfraStructure Network, <http://www.actris.net>).  
20 Located 20 km Southwest of Paris (2.15° E, 48.71° N, 150 m above sea level) in a semi-rural  
21 area, this atmospheric supersite is representative of the regional background pollution over the  
22 region of Paris (Haefelin et al., 2005; Crippa et al., 2013a).

23 The chemical composition of non-refractory submicron aerosol has been continuously  
24 monitored using a Quadripole Aerosol Chemical Speciation Monitor (Aerodyne Research  
25 Inc.) which has been described in details by Ng et al., (2011). Briefly, PM<sub>2.5</sub> aerosols are  
26 sampled at 3 L/min (from a PM<sub>2.5</sub> cyclone inlet) and then sub-sampled at 85 mL/min  
27 (volumetric flow) through an aerodynamic lens, focusing submicron particles (40 nm - 1000  
28 nm aerodynamic diameter, A.D.) onto a 600°C-heated conical tungsten vaporizer where non-  
29 refractory material are flash-vaporized and quasi-instantaneously ionized by electron impact  
30 at 70 eV. Fragments are detected following their mass-to-charge ratio by a quadrupole mass  
31 spectrometer. The procedure followed for the retrieval of chemical species concentrations  
32 from ACSM measurements is fully described in the Supporting Material. Briefly, the  
33 instrument calibration has been performed following the recommendation of Jayne et al.  
34 (2000) and Ng et al. (2011), where generated mono-disperse 300 nm A.D. ammonium nitrate  
35 particles are injected into both ACSM and Condensation Particle Counter (CPC) at different  
36 concentrations. Throughout the measuring period, three Response Factor (RF) calibrations  
37 and one (NH<sub>4</sub>)<sub>2</sub>SO<sub>4</sub> calibrations were performed, summarized in Table 1. The low drift of the  
38 obtained slopes allowed the use of an average response factor of  $2.72 \cdot 10^{-11}$  (with a standard  
39 deviation of  $\pm 13\%$ ), as well as relative ion efficiencies (RIE) of 5.9, 1.2 and 1.4 for  
40 ammonium, sulphate and organic matter respectively, were used for the whole dataset.



1 Collection efficiencies were corrected using algorithms proposed by Middlebrook et al.  
2 (2012), and data were finally cross-validated using collocated  $PM_1$  as well as  $PM_{2.5}$  urban  
3 background measurements, retrieved from the regional association of air quality monitoring  
4 (AIRPARIF, <http://airparif.asso.fr>). The  $PM_1$  and  $PM_{2.5}$  datasets were obtained using Tapered  
5 Element Oscillating Microbalances (TEOM) equipped Filter Dynamic Measurements Systems  
6 (FDMS) as described by Grover (2005). A comprehensive determination of the overall  
7 uncertainty (as well as  $PM_1$  components) associated to ACSM-derived measurements has  
8 been carried out in November 2013 through an inter-comparison exercise (Crenn et al., in  
9 preparation; Fröhlich et al., 2015). Here, the consistency of ACSM measurements has been  
10 assessed from the comparison with co-located measurements, as described in Section 3.

11 A total number of ~26,000 ACSM data points (with a temporal resolution of 30 min) were  
12 collected from June 2011 to June 2013 covering on average  $92 \pm 9\%$  of each month over this  
13 2-year period (it is to note that Sept-Oct 2012 and Feb-March 2013 were not taken into  
14 account within the latter calculation because the instrument was used for short-term intensive  
15 campaigns at other locations).

16 Aerosol light absorption coefficients  $b_{abs}$  were retrieved every 5 minutes from a 7-wavelength  
17 (370, 470, 520, 590, 660, 880 and 950 nm) AE31 Aethalometer from June 2011 to February  
18 2013, and from a 7-wavelength (370, 470, 520, 590, 660, 880 and 950 nm) AE33  
19 Aethalometer from February 2013 to May 2013. In both cases, instruments sampled aerosols  
20 with a  $PM_{2.5}$  cut-off inlet, operating at 5 L/min. Filter-based absorption measurements need to  
21 be compensated for multiple scattering in the filter matrix and for loading effects, using  
22 mathematical algorithms (Collaud Coen et al., 2010). While AE31 data were compensated  
23 using the corrections of Weingartner et al. (2003) as described in Sciare et al. (2011), the use  
24 of the Dual-Spot Technology® in the AE33 avoids the need of manual post-processing to  
25 compensate the data (Drinovec et al., 2014). Both instruments performed absorption  
26 measurements simultaneously during 7 days in February 2013 (Fig. S1a). Absorption  
27 coefficients at 880 nm showed a slope of 0.93 and a very satisfactorily  $r^2$  (0.96,  $n=3,023$  of 5-  
28 min data points). Black Carbon concentrations for the whole (2-year) dataset were then  
29 calculated from the absorption coefficient at 880 nm, with a mass absorption cross-section  
30 (MAC) of  $8.8 \text{ m}^2/\text{g}$  (Fig. S1b), determined from the comparison with collocated filter  
31 measurements of elemental carbon (EUSAAR2 thermo-optical protocol, Cavalli et al., 2010).  
32 This value is close to the default input value implemented in the AE33 at 880 nm ( $7.77 \text{ m}^2/\text{g}$ ).  
33 Although still under discussion (Bond and Bergstrom, 2006; Cappa et al., 2012), such  
34 relatively high MAC values might be related to a possible encapsulation of soot particle by  
35 organic/inorganic compounds at our regional background site and to the presence of BC from  
36 wood burning emissions during wintertime, both leading to an increase of BC mass  
37 absorption efficiency (Liousse et al., 1993; Bond and Bergstrom, 2006; Lack et al., 2008). A  
38 total number of ~280,000 BC data points (~133,000 5-min points from AE31 and ~147,000 1-  
39 min points from AE33) were collected from June 2011 to June 2013.

40 Ammonia measurements during selected periods (mainly during the spring, winter and  
41 summer seasons) were carried out using an AiRRmonia (Mechatronics Instruments BV, The  
42 Netherlands). Based on the conductimetric detection of ammonium, gaseous ammonia is

1 sampled at 1 L/min through a sampling block equipped with an ammonia-permeable  
2 membrane; a water counter-flow allows ammonia to solubilize in ammonium. A second  
3 purification step is applied by adding 0.5 mM sodium hydroxide, leading to the detection of  
4 ammonium in the detector block. The instrument has been calibrated regularly using solutions  
5 of 0 ppb and 500 ppb of ammonium. Two sets of sampling syringes ensure a constant flow  
6 throughout the instrument, but also create a temporal shift, estimated at 20 to 40 min by  
7 different studies (Cowen et al., 2004; Zechmeister-Boltenstern, 2010). In our case, this shift  
8 was set at 30 min.

9 Pre-fired 47-mm diameter quartz filters were sampled in PM<sub>2.5</sub> at the same location using a  
10 low-volume (1m<sup>3</sup>/h) sampler (Partisol Plus, Thermo Environment) equipped with a volatile  
11 organic compounds active charcoal denuder. Four-hour filters and 24-h filters were  
12 discontinuously sampled respectively from 10 Feb. 2012 to 02 Mar. 2012 and during the  
13 period from August 2012 to April 2013. These filters were analyzed for their water-soluble  
14 inorganic (anions and cations) and elemental/organic carbon contents using respectively Ion  
15 Chromatography and Sunset OC/EC analyzer (EUSAAR2 thermal protocol), accordingly to  
16 Sciare et al. (2008) and Cavalli et al. (2010).

17 Finally, standard meteorological parameters (Temperature, Relative Humidity, Wind Speed  
18 and Direction) were obtained from continuous measurements at Ecole Polytechnique, located  
19 4 km East of our station with an A100R Campbell Scientific cup anemometer for wind speed  
20 and a W200P weathervane for wind direction, at 10 m above ground level. Additionally, the  
21 Boundary Layer Height (BLH) was derived from Pal et al. (2013) methodology. The  
22 attribution of the BLH was processed in combining diagnostic of the surface stability from  
23 high frequency sonic anemometer measurements and LIght Detection and Ranging (LIDAR)  
24 attenuated backscatter gradients from aerosols and clouds.

25 All measurements presented here are expressed in Coordinated Universal Time (UTC).  
26 Seasons are differentiated upon seasonal equinoxes.

27

## 28 **2.2 Urban background PM<sub>2.5</sub> measurements**

29 Within the framework of mandatory air quality monitoring, urban background measurements  
30 are continuously being carried out in the region of Paris. Hourly PM<sub>2.5</sub> data from TEOM-  
31 FDMS measurements were retrieved from the three stations representative of the Paris urban  
32 background (namely Bobigny, Gennevilliers and Vitry-sur-Seine). Datasets are available  
33 online upon request on <http://airparif.asso.fr>.

34

## 35 **2.3 Backtrajectories and Non-parametric Wind Regression**

36 To illustrate air mass origin during specific pollution episodes, 72-h backtrajectories were  
37 calculated every 3 hours from the PC based version of Hysplit (Draxler, 1999) with GDAS

1 meteorological field data. Backtrajectories were set to end at SIRTA coordinates (48.71°N,  
2 2.21°E) at 100 m above ground level.

3 Non-parametric Wind Regression (NWR) is a smoothing algorithm (Henry et al., 2009) to  
4 alternatively display pollution roses, and has been already successfully applied to various  
5 atmospheric pollutants and pollution sources (Yu et al., 2004; Pancras et al., 2011; Olson et  
6 al., 2012). The objective is to estimate the concentration of a pollutant given any ( $\theta$ ,  $\vartheta$ ) couple  
7 (wind direction and speed, respectively), from measured wind speed and direction, and  
8 concentration.

$$E(\theta|\vartheta) = \frac{\sum_{i=1}^N K_1\left(\frac{\theta - W_i}{\sigma}\right) \cdot K_2\left(\frac{\vartheta - Y_i}{h}\right) \cdot C_i}{\sum_{i=1}^N K_1\left(\frac{\theta - W_i}{\sigma}\right) \cdot K_2\left(\frac{\vartheta - Y_i}{h}\right)}$$

9 Where E is the concentration estimate at a wind direction  $\theta$  and speed  $\vartheta$ ;  $W_i$ ,  $Y_i$  and  $C_i$  the  
10 wind direction, speed and atmospheric concentrations, respectively, measured at  $t_i$ ;  $\sigma$  and  $h$   
11 the smoothing factors; and  $K_1$  and  $K_2$  two kernel smoothing functions defined as:

$$K_1(x) = \frac{1}{\sqrt{2\pi}} \cdot e^{-0.5 \cdot x^2}, -\infty < x < \infty$$

$$K_2(x) = 0.75 \cdot (1 - x^2), -1 < x < 1 = 0$$

12 The choice of the two smoothing factors  $\sigma$  and  $h$  can be carried out using statistical  
13 calculations, although its empirical determination stays feasible, as final interpretation should  
14 not be changed. Here,  $\sigma$  and  $h$  were set to 7 and 1.5, similarly to Petit et al. (2014). Finally,  
15 the equivalent of the wind rose is calculated from the probability density:

$$f(\theta, \vartheta) = \frac{1}{N\sigma h} \cdot \sum_{i=1}^N K_1\left(\frac{\theta - W_i}{\sigma}\right) K_2\left(\frac{\vartheta - Y_i}{h}\right)$$

16 where N the is the total number of points.

17 Due to higher measurement uncertainties in wind direction at low speeds, data associated with  
18 wind speeds lower than 1 m/s were discarded, potentially inducing an underestimation of very  
19 local pollution events.

20

## 21 **2.4 Source apportionment of carbonaceous aerosols**

22 The measurement of aerosol absorption at multiple wavelengths is allowing for BC source  
23 apportionment. Organic molecules, especially Polycyclic Aromatic Hydrocarbons and Humic-  
24 Like Substances, strongly absorb in the UV and blue part of the light spectrum. Based on the  
25 fact that these compounds are primarily related to biomass combustion, the deconvolution of  
26 BC into two contributions: fuel fossil and wood burning ( $BC_{ff}$  and  $BC_{wb}$ , respectively) can be  
27 carried out (Sandradewi et al., 2008). Such source apportionment has already been

1 successfully performed during intensive field campaigns as well as for long-term monitoring  
2 periods, frequently enlightening the significant contribution of wood burning to ambient BC  
3 concentrations during wintertime (Favez et al., 2009, 2010; Sciare et al., 2011, Herich et al.,  
4 2011; Crippa et al. 2013a). Here, the 470 nm and 880 nm channels were used, with an  
5 absorption Ångström exponent of 2.1 and 1.0 for pure wood burning and traffic, respectively,  
6 similarly to previous work focusing on the February-March 2012 period of the same dataset  
7 (Petit et al., 2014).

8 The source apportionment of our organic aerosol data is not presented here although Positive  
9 Matrix Factorization applied to AMS or ACSM database is an efficient tool for the  
10 identification of organic aerosol primary sources and secondary formation processes (see for  
11 instance Lanz et al., 2007; Jimenez et al. 2009; El Haddad et al., 2013; Carbone et al., 2013;  
12 Bougiatioti et al., 2014; Petit et al. 2014). Such a work will be reported elsewhere (Crenn et  
13 al., in prep.) as important issues related to the seasonal variation of specific organic aerosol  
14 factor profiles have to be addressed in many details with a lot of sensitivity tests which are  
15 beyond the objectives of the present study.

16

### 17 **3. Cross-validation of particulate chemical species concentrations**

18 Fig. 1 illustrates the temporal variations of chemical species concentrations used for the  
19 present study from June 2011 to May 2013. This extended duration highlights the robustness  
20 of used instruments, and in particular the ACSM which did not undergo any major failures  
21 over this 2-year period. The consistency of the concentrations of each chemical constituent  
22 retrieved from the ACSM has been checked via comparisons with filter measurements (Fig. 2)  
23 as well as a chemical mass closure of PM<sub>1</sub> (Fig. 3).

24 ACSM nitrate is very consistent with filter measurements, the slope of the linear regression  
25 being close to 1 ( $r^2=0.85$ ,  $N=147$ ). No overestimation of ACSM nitrate is observed at high  
26 concentrations, which suggests the ability of the Middlebrook algorithm to properly correct  
27 our ACSM collection efficiencies. Higher discrepancies are observed for sulphate. This  
28 feature has already been mentioned in previous studies for ACSM (Ng et al., 2011;  
29 Budisulistiorini et al., 2014), and AMS instruments (Takegawa et al., 2005). This could be  
30 partly related to the size distribution of sulphate, as fine (PM<sub>2.5</sub>) sulphate can partially be  
31 associated with submicron sea salt and/or dust particles. Fine ammonium sulphate aerosols  
32 originating from secondary processes and long-range transport (Sciare et al., 2010; Freutel et  
33 al., 2013) may also present a larger size mode extending above 1  $\mu\text{m}$  and partially not  
34 sampled by the ACSM. A sulphate ion efficiency calibration was also performed in May 2013  
35 to investigate possible change in RIE, but no significant discrepancy from the default value of  
36 1.2 was found.

37 The OM-to-OC ratio obtained from the comparison between ACSM and filter-based  
38 measurements exhibits a mean value of approximately 1.5, which is lower than the value  
39 recommended for urban areas ( $1.6 \pm 0.2$ , Turpin and Lim, 2001) and 33% lower than and/or  
40 equal to values used in Paris metropolitan area in previous studies ( $\sim 2$  in Bressi et al., 2013;

1 1.6 in Sciare et al., 2010). Although this ratio is subject to caution, by virtue of potential  
2 geographical and temporal discrepancies, the relatively low value observed here might be  
3 explained by the presence of organic material between 1 and 2.5  $\mu\text{m}$  as well as filter sampling  
4 artifacts.

5 A chemical mass closure exercise, where the combination of validated ACSM and  
6 Aethalometer data is compared to co-located  $\text{PM}_{10}$  TEOM-FDMS measurements, was used to  
7 assess the capacity of the two former instruments to correctly describe the  $\text{PM}_{10}$  fraction over  
8 long-term periods. For this purpose, the reconstructed  $\text{PM}_{10}$  ( $\text{PM}_{\text{chem}}$ ) introduced here  
9 corresponds to the sum of all non-refractory species measured by the ACSM ( $\text{OM}$ ,  $\text{NO}_3^-$ ,  
10  $\text{SO}_4^{2-}$ ,  $\text{NH}_4^+$  and  $\text{Cl}^-$ ) and Black Carbon measured by Aethalometer, and is assumed to quasi-  
11 exhaustively account for submicron aerosols (Putaud et al., 2004).  $\text{PM}_{\text{chem}}$  daily averages  
12 were compared to the TEOM-FDMS dataset, since the latter instrument is considered as  
13 equivalent to the gravimetric reference method on this temporal scale. From June 2011 to  
14 May 2013, the 341-point (this number being due to the combined availability of ACSM, BC  
15 and PM data) scatter plot shows a very satisfactory correlation coefficient ( $r^2=0.85$ ) with a  
16 slope of 1.06.

17

#### 18 **4. Representativeness of our 2-year observation period**

19 Monthly mean atmospheric conditions were compared to standard meteorological parameters  
20 in order to investigate any anomalies over the 2011-2013 period (Fig. 4). Temperature,  
21 rainfall and sun exposure representative for the region of Paris were retrieved from monthly  
22 weather reports available at <https://donneespubliques.meteofrance.fr>, and are calculated from  
23 a 30-year period (1981-2010) (Arguez and Vose, 2011). A similar study was also performed  
24 for particulate matter concentrations, with representative  $\text{PM}_{2.5}$  defined as the average  $\text{PM}_{2.5}$   
25 concentrations calculated from 2007 to 2014 at the three historical Airparif urban background  
26 stations.

27 Briefly, autumn 2011 was relatively mild,  $\text{PM}_{2.5}$  levels being close to representative  
28 concentrations for the period. The end of winter 2011-2012 and early spring 2012 were  
29 particularly dry and sunny, enabling enhanced photochemical transformation and exhibited  
30 unusually high  $\text{PM}_{2.5}$  concentrations in February and March 2012. The summer 2012 was  
31 chilly and rainy, especially in June 2012, leading to lower  $\text{PM}_{2.5}$  levels (Yiou and Cattiaux,  
32 2013). Finally, the first two months of 2013 were unusually cold, whereas March 2013 was  
33 remarkably representative of wintertime conditions. The highest observed discrepancies occur  
34 with highest measured mass, which may highlight an intensification of pollution episodes. On  
35 a broader perspective, this feature is also observed through inter-annual variability of urban  
36 background  $\text{PM}_{2.5}$  concentrations (Fig. S2). This underlines the need of continuous  
37 monitoring over several year periods. Interestingly, no direct link can be drawn between  
38 meteorological anomalies and unusual high  $\text{PM}_{2.5}$  concentrations. Indeed, while the high  
39  $\text{PM}_{2.5}$  levels observed in Feb. 2012 and March 2012 may be linked to unusual low  
40 temperatures, exceptionally high temperatures can also be associated with high  $\text{PM}_{2.5}$   
41 concentrations. This has to be related to the seasonal variability of sources, origins and

1 (trans)formation pathways; and is being investigated within the following sections, taking  
2 advantage of long-term trend analysis, wind regression, diurnal variations, and the analysis of  
3 pollution episodes.

4 Finally, it should be underlined that the Paris region is mostly influenced by winds coming  
5 from the Southwest (Fig. 5) sector. This sector is characterized by clean air masses from the  
6 Atlantic Ocean with high wind speeds, and is usually associated with low PM concentrations.  
7 The Northeast wind sector exhibits a smaller occurrence than previously observed between  
8 Sept. 2009 and Sept. 2010 (Supplementary information of Bressi et al., 2013).

9

## 10 **5. Long-term trend and general features**

11 2-year temporal variations of the chemical composition of submicron aerosols (OM,  $\text{NO}_3^-$ ,  
12  $\text{SO}_4^{2-}$ ,  $\text{NH}_4^+$ , Cl<sup>-</sup>,  $\text{BC}_{\text{ff}}$  and  $\text{BC}_{\text{wb}}$ ) and ammonia ( $\text{NH}_3$ ) are presented in Fig. 1. Similarly to  
13 Bressi et al. (2013), a clear seasonal pattern is observed here, with highest concentrations  
14 observed during winter and early spring while summer periods exhibit the lowest pollution  
15 levels (Fig. 6a), which is also consistent with general patterns observed in Northern Europe  
16 (Barnpadimos et al., 2012; Waked et al., 2014). Regardless of the season, OM dominates the  
17  $\text{PM}_{10}$  chemical composition, followed by ammonium nitrate whose contribution is highest  
18 during spring, a feature that is generally observed for European urban areas (Zhang et al.,  
19 2007; Putaud et al., 2010). Fig. 6b presents the binned major chemical composition and the  
20 frequency per season of data points as a function of  $\text{PM}_{10}$  concentration levels. The  
21 contribution of Secondary Inorganic Aerosols (SIA, mostly  $\text{NO}_3^-$ ,  $\text{SO}_4^{2-}$  and  $\text{NH}_4^+$ ) increases  
22 with the increases of  $\text{PM}_{10}$  mass until  $50 \mu\text{g}/\text{m}^3$ , highlighting the role of inorganic secondary  
23 pollution during spring months (Fig. 6b). This well-documented pattern that has already been  
24 reported for the region of Paris in several studies (see for instance Sciare et al., 2010 and  
25 Bressi et al., 2013a). Very interestingly, above  $50 \mu\text{g}/\text{m}^3$ , organic contribution, as well as  
26 wintertime frequency, increases to dominate the chemical composition of the highest  
27 measured  $\text{PM}_{10}$  concentrations with an associated increase in BC, a feature which has not been  
28 seen during the AIRPARIF-Particules projects, essentially due to highly time resolved  
29 measurements, nor investigated during the MEGAPOLI project. There are well defined  
30 occurrences of high concentrations ( $\sim 150$  data points of 30 min) suggesting sharp pollution  
31 events with a limited temporal duration; contradictorily to the  $20\text{-}50 \mu\text{g}/\text{m}^3$  mass class  
32 presenting much more data points that highlight either a higher frequency of sharp events  
33 and/or pollution episodes with a longer temporal duration.

34 We have used here the  $\text{BC}/\text{SO}_4$  ratio to assess potential transport of pollution. Sulphate  
35 mainly forms through heterogeneous processes with a slow kinetic rate and spreads over large  
36 scales (Putaud et al., 2004). For that reason, it can be considered as a good indicator of long-  
37 range transport assuming minor local  $\text{SO}_2$  sources (background annual  $\text{SO}_2$  concentrations of  
38 about  $2 \mu\text{g}/\text{m}^3$  in the region of Paris; AIRPARIF, 2014). On the contrary, Black carbon in the  
39 region of Paris shows an important gradient from the city center to regional background  
40 (Bressi et al., 2013a) and can be used to better infer local (Paris city) influence at our  
41 background station. Although in-situ sulphate formation may occur (for instance during fog

1 episodes; Healy et al., 2012) and long range transport of BC may be observed over the region  
2 of Paris (Healy et al., 2012 and 2013), as a whole, the use of the BC/SO<sub>4</sub> ratio may support  
3 our study on local / regional / advected pollution. As shown in Fig. 7, the BC/SO<sub>4</sub> ratio  
4 decreases along with the increase of PM<sub>1</sub> (and thus secondary ions mass fraction), suggesting  
5 potential regional and/or trans-boundary transport, and large-scale pollution episodes, as  
6 previously reported by several studies in Northern France (Bessagnet et al., 2005; Sciare et  
7 al., 2010; Bressi et al., 2013; Waked et al., 2014; Freutel et al., 2013). Very interestingly, this  
8 BC/SO<sub>4</sub> ratio dramatically increases for the highest concentrations, where the concomitant  
9 increases of the Ångström exponent, of the contribution of BC<sub>wb</sub> relatively to BC, along with  
10 the increase of OM and wintertime frequency (Fig. 7), suggest intense local and/or regional  
11 wood burning pollution episodes during winter. Moreover, except the single wood-burning  
12 episode observed on 5 Feb. 2012 (described in Petit et al., 2014) all these intense PM  
13 pollution peaks (PM<sub>1</sub> > 60 µg/m<sup>3</sup>) also occurred in most of the rural/suburban/urban  
14 AIRPARIF monitoring stations. This pattern underlines homogeneous meteorological  
15 conditions over the region of Paris with “local” emissions being measured at a regional scale  
16 (within a distance of at least 50 km from the city center).

17

## 18 **6. Seasonality and insights on geographical origins**

19 Fig. 8 displays the Wind Regression analysis plots for species of interest, naming OM, NO<sub>3</sub><sup>-</sup>,  
20 SO<sub>4</sub><sup>2-</sup>, NH<sub>3</sub>, BC<sub>ff</sub> and BC<sub>wb</sub>.

21 Overall, OM concentrations do not exhibit a particular dependence on wind direction, the  
22 regional background always staying at a significant contribution throughout seasons (~ 3-6  
23 µg/m<sup>3</sup>). However, higher OM concentrations occurred in autumn and winter and are  
24 associated with very low wind speeds suggesting higher local influence together with higher  
25 local wood burning emissions (as previously suggested from Fig. 6b and 7). During summer,  
26 OM concentrations are lower (by a factor of ~ 2.2) and show a more homogeneous  
27 distribution (e.g. with lower local influences).

28 As expected, semi-volatile nitrate concentrations are higher during the coldest months (in  
29 spring and winter). They are associated with relatively high wind speeds (~20 km/h) coming  
30 from the N and NE direction, suggesting significant medium-to-long-range transport of  
31 ammonium nitrate during these seasons which is consistent with similar observations reported  
32 for the region of Paris (Bressi et al., 2013a; Freutel et al., 2013; Petetin et al., 2013).  
33 However, the significant nitrate concentrations observed for all the range of wind speed from  
34 the N-NE direction suggest, at least for the lowest wind speed, a significant contribution of  
35 the region of Paris. Possible impacts of industrial activities in the Seine estuary (i.e. Rouen,  
36 Le Havre), especially during spring, may also be responsible for the noticeable nitrate hotspot  
37 observed in the NW sector. In autumn, nitrate concentrations are higher at low wind speeds,  
38 in agreement with the fact that traffic emissions are slightly higher in September and October  
39 than the rest of the year in Paris (V-Traffic report, 2014), and that BC<sub>ff</sub> concentrations are also  
40 the highest during these months. This is also consistent with a relatively fast nitrate formation  
41 mechanism from local NO<sub>x</sub> emissions as reported by Petetin et al. (2013).

1 Sulphate features different behaviour than nitrate, where the non-local origin is much more  
2 pronounced. High concentrations are associated with high wind speeds originating from the  
3 NNE, leading to the same conclusions as those reported in the literature on the major role of  
4 long range transport of this compound (Pay et al., 2012; Bressi et al., 2013b; Petetin et al.,  
5 2013; Waked et al., 2014). Petrochemical and shipping activities may explain the observed  
6 hotspot in the marine NW sector, especially noticeable in spring, which may be linked with  
7 meteorological conditions enhancing ammonium sulphate formation and transport.

8 The region of Brittany, located less than 300 km West of the region of Paris, is the principal  
9 emitter of ammonia in France through intense agricultural activities  
10 (<http://prtr.ec.europa.eu/DiffuseSourcesAir.aspx>). However, no clear contribution from this  
11 region is observed from our wind regression analysis. This may be partly related to very few  
12 occurrences of air masses passing over Brittany and reaching the region of Paris. Despite  
13 hotspots from the NE/E in spring, or from the N/NE in winter, no clear wind sector is directly  
14 responsible for high NH<sub>3</sub> concentrations at our station, suggesting a diffuse regional source  
15 for this compound.

16 In Europe, BC<sub>ff</sub> is assumed to be an excellent tracer of traffic emissions in urban areas  
17 (Herich et al., 2011 for instance). Although long range transported BC<sub>ff</sub> may not be excluded  
18 as shown by Healy et al. (2012, 2013), here, wind regression analyses show that high BC<sub>ff</sub>  
19 concentrations occurred at low wind speeds, highlighting the importance of local/regional  
20 traffic emissions in the Paris region, especially during the autumn and winter seasons. In  
21 spring, a clear distribution over a large range of wind speeds is noticeable in the NNE wind  
22 sector. This is consistent with the fact that Paris city is located NNE from our station (e.g.  
23 higher contribution of the Paris city plume to measured BC<sub>ff</sub> concentrations at SIRTA). This  
24 is also related to a higher occurrence of this wind sector during spring.

25 Black Carbon from biomass burning combustion (BC<sub>wb</sub>) presents a clear seasonal trend  
26 similar to OM, with the highest concentrations during cold seasons at low wind speeds,  
27 suggesting increasing local influence in wood burning emissions. The lowest boundary layer  
28 heights (BLH) observed during wintertime favouring the accumulation of pollutants at ground  
29 level together with the large contribution of individual (domestic) wood burning sources  
30 homogeneously spread over the region of Paris may explain the significant contribution of  
31 regional emissions observed during winter.

32 Finally, it should be noted that the geographical origin of each investigated chemical  
33 constituent remains globally unchanged throughout the year with a well-defined sectorized  
34 location. While SIA and BC<sub>ff</sub> fractions are mainly associated with the NNE sector (coming  
35 from Paris City and/or further away), highest OM and BC<sub>wb</sub> concentrations exhibit strong  
36 local NW and SE sectors origins. Various sources of organic matter also contribute to a  
37 significant contribution of the (unsectorized) regional background.

38

## 39 **7. Weekly diurnal profiles and insight on sources and processes**



1 Near real-time observations over long-term periods offer a unique opportunity to provide  
2 robust diurnal profiles for each season. First, Fig. 9 shows the average diurnal profiles of  
3 ambient temperatures (Fig. 9a) and BLH (Fig. 9b) across seasons. Weekly diurnal profiles for  
4 OM,  $\text{NO}_3^-$ ,  $\text{NH}_4^+$ ,  $\text{NH}_3$ ,  $\text{BC}_{\text{ff}}$  and  $\text{BC}_{\text{wb}}$  are presented for different seasons from hourly  
5 averages (Fig. 10). Sulphate variations are not presented and discussed here because they lead  
6 to poor daily variations (average of  $0.75 \mu\text{g}/\text{m}^3 \pm 2\%$ ), which are consistent with its mid-to-  
7 long range transport origin.

8 Clear weekly and diurnal patterns can be observed for carbonaceous aerosols. Independently  
9 to the investigated season,  $\text{BC}_{\text{ff}}$  presents a well-marked bimodal diurnal profile, with maxima  
10 in the morning (starting at 06:00 UTC) and the evening (starting at 17:00). This reflects the  
11 proximity of the traffic source (with daily commuting) and dilution in the boundary layer  
12 during daytime (Fig. 9b). With an average of  $0.61 \mu\text{g}/\text{m}^3$ , weekdays exhibit slightly higher  
13 concentrations than weekends ( $0.51 \mu\text{g}/\text{m}^3$  on average). By comparison, the diurnal variability  
14 of  $\text{BC}_{\text{wb}}$  is revealed only in autumn and winter, with the combination of enhanced wood  
15 burning emissions, low temperatures and BLH (Fig. 9), leading to a unimodal pattern with  
16 increasing concentrations after 18:00 UTC. Although individual wood-burning stoves only  
17 represent around 5% of the means of heating in the region of Paris, they contribute to almost  
18 90% of  $\text{PM}_{10}$  residential emissions in the region of Paris (Airparif emission inventory for the  
19 year 2010; Airparif, 2013) and are likely to represent the major contributor to  $\text{BC}_{\text{wb}}$ .

20 For OM, highest variations (in terms of concentration amplitude) are observed during autumn  
21 and winter, with a growing influence of wood-burning heating, as OM concentrations nicely  
22 follow  $\text{BC}_{\text{wb}}$  ones. Levels of both compounds during the evening are approximately 20%  
23 higher during weekends than during weekdays. More specifically, low BLH in winter  
24 (Fig. 9b) increase measured concentrations, leading, for example, to morning OM peaks that  
25 should be linked to traffic emissions. By contrast, the diurnal profile is rather flat with poor  
26 temporal variations in summer and is accordance with the homogeneous geographical  
27 distribution from NWR calculation for this season. The lack of decrease in the afternoon  
28 during weekdays suggests rapid formation of secondary organic aerosols (SOA) from diverse  
29 anthropogenic (traffic for instance, as underlined by Platt et al., 2013 and Nordin et al., 2013)  
30 and biogenic sources (Carlton et al., 2009). During spring, OM globally follows the variations  
31 of nitrate, highlighting fast displacements of gas-particle equilibriums of semi-volatile  
32 material due to meteorological conditions. Some peaks are observed some days during the  
33 night, which could underline the residual contribution of wood burning emissions in March  
34 and April.

35 For SIA, nitrate and ammonium display very similar diurnal and weekly profiles, illustrating  
36 the importance of ammonium nitrate by comparison with ammonium sulphate. Both  
37 compounds display well-marked diurnal profiles with maximum at night (especially in  
38 autumn and winter) and/or early morning (especially in spring and summer), which has to be  
39 related to the enhancement of ammonium nitrate formation under low temperature and/or high  
40 relative humidity. The temporal variations of the two compounds can also be linked to the one  
41 of ammonia. For instance, during summertime, ammonia presents unimodal diurnal profiles,  
42 with highest values around noon, and nicely follows temperature (Fig. 9a), in good agreement

1 with previous studies (Bari et al., 2003; Lin et al., 2006). This phenomenon is exactly  
2 opposite to the variations of ammonium and nitrate exhibiting unimodal pattern with highest  
3 concentrations during the night. Meteorological conditions can then fully explain the  
4 formation/partitioning of SIA as well as ammonia concentration during summer.

5 Interestingly however, ammonia shows different profiles as a function of the season. In  
6 particular, during springtime, this compound displays a clear bimodal profile, with a morning  
7 and an evening peak, concomitant with traffic emissions and that come over elevated regional  
8 background levels due to the use of nitrogen-containing fertilizers in this period of the year.  
9 However, this bimodal pattern is not observed during the summer and winter seasons, where  
10 traffic also occurs. Although traffic-related ammonia has already been reported in urban  
11 environments (Edgerton et al., 2007; Pandolfi et al., 2012; Saylor et al., 2010) and several  
12 studies raising concerns about uncontrolled ammonia emissions from De-NO<sub>x</sub> systems (Baum  
13 et al., 2001; Heeb et al., 2006 and 2012 for instance), this spring bimodal profile may also be  
14 related to other parameters than traffic emissions. Indeed, as already described by Bussink et  
15 al. (1996), emission of ammonia can occur during the evaporation of the morning dew,  
16 especially when soils are loaded with fertilizers. The morning decrease observed for ammonia  
17 in spring can then be associated with the growing of the mixing depth layer (Fig. 9b) while, in  
18 the afternoon ammonia increases may be partly explained by temperature driven gas-phase  
19 partitioning changes of ammonium nitrate.

20

## 21 **8. PM<sub>1</sub> pollution episodes over the region of Paris**

22 An in-depth characterization of each pollution episodes over the region of Paris is particularly  
23 important in the context of mitigation policies which are usually taken at a local scale during  
24 these episodes. Such investigation should provide useful information regarding PM  
25 (trans)formation processes and help identifying parameters influencing the temporality of  
26 their chemical composition.

27 Statistical representativeness of pollution episodes (duration and intensity) may be addressed  
28 using our long-term datasets. Based on our 2-year dataset, the highest 1% of observed PM<sub>1</sub>  
29 concentrations ( $q_{99} \sim 49 \mu\text{g}/\text{m}^3$ , representing around 200 data points of 30min; i.e.  
30 approximately 100h) mostly occur during February, April and November, while persistent  
31 pollution episodes (PM<sub>1</sub> > 20  $\mu\text{g}/\text{m}^3$  during at least 3 consecutive days) mostly occur in early  
32 Spring. More interestingly, the majority of the highest PM<sub>1</sub> concentrations fall within these  
33 persistent pollution episodes. As previously suggested from higher BC/SO<sub>4</sub> ratios (Section 5  
34 and Fig. 7), the highest PM<sub>1</sub> concentration peaks are associated with rather local emissions.  
35 This result clearly points to the contribution of local/regional emissions during persistent  
36 pollution episodes. A more detailed analysis (episode-by-episode) is performed in the  
37 following to better characterize the local/regional versus advected PM pollution during  
38 persistent pollution episodes.

39 Eight persistent pollution episodes (PM<sub>1</sub> > 20  $\mu\text{g}/\text{m}^3$  during at least 3 consecutive days) were  
40 detected between mid-2011 to mid-2013 and are displayed in Table 2 and Fig. 12&13. Fig. 12

1 shows the averaged PM<sub>1</sub> chemical composition (in µg/m<sup>3</sup>) for each episode, chronologically  
2 numbered, from 1 to 8. Table 2 summarizes key information for each episode. Fig. 13 shows  
3 air masses origins, wind rose and temporal variations of the chemical composition of each  
4 episode. As a general pattern for each episode, the chemical composition of PM<sub>1</sub> is dominated  
5 by OM and/or ammonium nitrate. Sulphate presents the highest variability (concentration  
6 standard deviation of 53% over all episodes) compared to OM and nitrate (~30%), possibly  
7 suggesting various contributions of advected pollution.

8 The following provides a thorough description of each episode.

9 Episode 1 (19/11/2011 – 24/11/2011): While winds come from the NW and E sectors, 72h-  
10 backtrajectories originate from SSE and exhibit a recirculation over a part of the Northern  
11 France. Moreover, along with the BC/SO<sub>4</sub> ratio (3.56; e.g. the highest of all episodes), and a  
12 low BLH with no significant variations, the chemical composition is largely dominated by  
13 OM (60.8% of PM<sub>1</sub>), suggesting significant local influence. The contribution of BC<sub>wb</sub> remains  
14 insignificant compared to BC<sub>ff</sub>, which could underline the accumulation in the atmosphere of  
15 fossil-fuelled combustion sources (notably illustrated by the very low altitude of the air  
16 masses ending on the 21 and 23 Nov).

17 Episode 2 (05/02/2012 – 13/02/2012): This episode presents two distinct phases. At the  
18 beginning, air masses come from the SE but originating from the E at low altitudes; along  
19 with very low temperatures (below 0°C all day), high OM and BC concentrations and BC/SO<sub>4</sub>  
20 ratio (average of 22.6 and 0.6 µg/m<sup>3</sup>, and 2.7, respectively from 5 to 8 Feb.). This is related to  
21 an intense local wood-burning episode, already thoroughly described in Petit et al. (2014).  
22 Then, from the 8 Feb, winds and air masses originate from NNE and secondary inorganic  
23 ions, especially ammonium nitrate, dominate the chemical composition. The associated wind  
24 speed may underline mid- to long-range transport, although the impact of the Paris plume  
25 cannot be excluded here.

26 Episode 3 (29/02/2012 – 03/03/2012): Along with this pollution episode, trajectories have  
27 rapidly changed in origin but have remained low in altitude. The RH remained very high,  
28 reaching 100% most of the time. Very interestingly, concentrations dropped on 01/03 and  
29 03/03 during the beginning of the day, coinciding with two stratus lowering fog events. These  
30 two fog events occurred during the second half of the night, and evaporated as the sun rose.  
31 The influence of fogs regarding the chemical transformation of PM<sub>1</sub> is notably highlighted by  
32 higher sulphate concentrations just after the evaporation of the first fog (and also when  
33 trajectories flew over the English Channel and Belgium), which could suggest transported  
34 SO<sub>2</sub> and oxidation over the region of Paris enhanced by fast fog processing (Kai et al., 2007;  
35 Rengarajan et al., 2011).

36 Episode 4 (12/03/2012 – 17/03/2012): Winds have originated from all directions (but mostly  
37 from NNE) suggesting anticyclonic conditions. The first half of the period exhibits rather  
38 stable chemical composition (dominated by ammonium nitrate) and clear diurnal variations of  
39 RH, T and BHL. Then, after 15/03, daily amplitudes of the following 3 meteorological  
40 parameters increased: T reached 20°C, RH 30% and BHL 1000 m, compared to the first half  
41 where they reached 15°C, 50% and 600m, respectively. This caused rapid decreases of

1 concentrations, due to higher temperature amplitudes enhancing the gas partitioning of semi-  
2 volatile material, and an increase of BLH allowing the dilution of atmospheric pollutants.

3 Episode 5 (23/03/2012 – 26/03/2013): Air masses originated from the NE to the E, and winds  
4 from the N to the NE. This episode is characterized by the strong diurnal variation of OM and  
5 ammonium nitrate, due the high amplitude of the BLH and temperatures going above 15°C,  
6 similarly to the previous episode. The high average BC/SO<sub>4</sub> ratio (2.37) is not representative  
7 of its temporality; the highest values are observed for lowest PM concentrations (26/03  
8 afternoon). With this exception, low BC/SO<sub>4</sub> values (< 1), and the chemical composition  
9 dominated by ammonium nitrate suggest mid and/or long-range transport.

10 Episode 6 (28/03/2012 – 31/03/2012): It exhibits the same behaviour than episode 5 with a  
11 clear medium-to-long range origin pattern (wind speed ~ 10 km/h, chemical composition  
12 dominated by ammonium nitrate), but with backtrajectories coming from NW/NE. Low  
13 altitude of backtrajectories illustrate the accumulation of pollutants along the trajectory of the  
14 air masses. However, the BC peak on the 30 Mar. morning (the high BC<sub>ff</sub> fraction suggests  
15 traffic emissions) could underline an influence of the Paris plume.

16 Episode 7 (16/01/2013 – 21/01/2013): Air masses display a coiling pattern around Northern  
17 France. The BC/SO<sub>4</sub> ratio, remaining lower than 1, suggests advected pollution. However, the  
18 strong variability of BC<sub>wb</sub> illustrates a significant influence of wood-burning emissions. No  
19 BHL data are available during this episode, but the altitude of backtrajectories may underline  
20 a more important dilution of the pollution.

21 Episode 8 (01/04/2013 – 08/04/2013): This episode actually started in 22/03, but no ACSM  
22 data were available at that time; however, meteorological conditions from 22/03 to 01/04  
23 were very similar, notably in terms of wind speeds and direction. It is characterized by air  
24 masses originating from the NE and a very low BC/SO<sub>4</sub> ratio, illustrating a typical case of  
25 advected secondary pollution, clearly dominated by ammonium nitrate and sulphate.

26 Overall, the observed variability, in terms of meteorological conditions, air mass origins, and  
27 chemical composition illustrates the variety of persistent pollution episodes, in terms of PM  
28 sources and different geographical origins. The BC/SO<sub>4</sub> ratio has shown to represent a useful  
29 tool to assess the local/regional/advected dimension of a specific pollution episode. Indeed,  
30 high ratios ( $\geq 2$ ) are usually associated with accumulation of local and/or regional emissions,  
31 while very low ratios ( $\leq 0.5$ ) are more representative of secondary advected pollutants. Ratios  
32 within this range should then be associated with a combined influence of regional and  
33 advected pollution. Finally, artefact-free ACSM data have shown to be adequate to document  
34 semi-volatile aerosols (ammonium nitrate and a fraction of OM), which strongly contribute to  
35 PM<sub>1</sub> during persistent pollution episodes, and real-time measurements allow to illustrate the  
36 close interactions between the chemical composition and meteorological parameters  
37 influencing its temporality.

38

## 39 9. Conclusions

1 The chemical composition of submicron ( $PM_{10}$ ) aerosols was continuously monitored in near  
2 real-time at a regional background site of the region of Paris between June 2011 and May  
3 2013 using a combination of an ACSM and an Aethalometer. The obtained 2-year dataset  
4 allows an appraisal of the robustness of ACSM measurements over several month periods, as  
5 well as Aethalometer measurements and BC source apportionment.

6 Non-parametric Wind Regression calculations has been performed for each season and  
7 provided useful information regarding the geographical origin of  $PM_{10}$  chemical constituents.  
8 SIA, in particular ammonium sulphate, show a clear advected pattern, leading to a uniform  
9 signal over large scales. Ammonium nitrate also exhibits a significant contribution of regional  
10 and local emissions. The highest concentrations of OM were identified as having a major  
11 local origin, while regional background OM concentrations remain significant, especially in  
12 spring and summer. The region of Brittany (Western France), the major hotspot of ammonia  
13 in France, seems to have little influence on the concentrations of this species at our station in  
14 the region of Paris; overall regional background concentrations of ammonia dominate,  
15 especially in Spring. Similarly to OM, wintertime  $BC_{wb}$  concentrations are mainly from local  
16 emissions from domestic heating although a noticeable regional background is still observed  
17 for this tracer of wood burning. As expected,  $BC_{ff}$  shows a clear local (nearby) origin, as well  
18 as contribution from the Paris city plume, and remains fairly constant throughout seasons, due  
19 to its regional traffic origin.

20 Such near real-time observations over long-term periods offer a unique opportunity to provide  
21 robust diurnal profiles for each season. For instance, diurnal profiles of semi-volatile nitrate  
22 aerosols were observed in different seasons with temperatures favouring its partitioning into  
23 the particulate phase in the morning and in the gas phase in the afternoon. No clear  
24 contribution of traffic could be proven regarding ammonia variability, and the regional  
25 background seems to prevail.

26 All the persistent pollution episodes ( $PM_{10} > 20 \mu g/m^3$  during at least 3 consecutive days)  
27 which occurred between 2011 and 2013 were carefully examined showing different  
28 meteorological conditions, sources and geographical origins making it difficult to draw  
29 general rules for these episodes. The  $BC/SO_4$  ratio was used here to better separate local,  
30 regional (BC dominated) and advected ( $SO_4$  dominated) contributions, and showed that, with  
31 very few exceptions, most of these persistent episodes were dominated by medium-to-long  
32 range transported pollution. However, it is interesting to note that the majority of the highest  
33 (time-limited)  $PM_{10}$  concentrations (30-min ACSM data points with  $PM_{10} > 50 \mu g/m^3$ ) fell  
34 within these persistent pollution episodes and were characterized by a significant  
35 local/regional contribution (high  $BC/SO_4$  ratios). This result, obtained with real-time  
36 measurements, may offer new perspectives in the definition and the evaluation of the  
37 effectiveness of local mitigation policies such as emergency measures (traffic or wood  
38 burning restrictions, for instance) taken to improve air quality during pollution events. In  
39 parallel, the long-term characterization of the organic fraction would surely lead to a better  
40 assessment of aerosol sources and some (trans-)formation processes of secondary pollution in  
41 the Ile-de-France area.

1

2 In conclusion, these first 2-year quality-controlled measurements of ACSM clearly  
3 demonstrate their great potential to monitor on a long term basis aerosol sources and their  
4 geographical origin and provide strategic information in near real-time during pollution  
5 episodes. They also support the capacity of the ACSM to be proposed as a robust and credible  
6 alternative to filter-based sampling techniques for long term monitoring strategies. The  
7 networking of such instrumentation (ACSM and BC) throughout Europe – as currently being  
8 built up within the European ACTRIS program - will certainly offers tremendous  
9 opportunities for modeling studies in order to improve prevision models, as well as large scale  
10 spatially and temporally resolved source apportionment studies of organic aerosols using the  
11 high potential of ACSM organic fragments.

12

13

#### 14 **Acknowledgments**

15 The research leading to the these results has received funding from INERIS, CNRS, CEA, the  
16 French SOERE-ORAURE network, the European Union Seventh Framework Program  
17 (FP7/2007-2013) project ACTRIS under grant agreement n°262254, the DIM-R2DS program  
18 for the funding of the ACSM equipment, the PRIMEQUAL-PREQUALIF and ADEME-  
19 REBECCA programs for the long term observations of Black Carbon at SIRTA.

20

## 1 **References**

- 2 Aiken, A. C., Salcedo, D., Cubison, M. J., Huffman, J. A., DeCarlo, P. F., Ulbrich, I. M.,  
3 Docherty, K. S., Sueper, D., Kimmel, J. R., Worsnop, D. R. and others: Mexico City aerosol  
4 analysis during MILAGRO using high resolution aerosol mass spectrometry at the urban  
5 supersite (T0)–Part 1: Fine particle composition and organic source apportionment,  
6 *Atmospheric Chem. Phys.*, 9(17), 6633–6653, 2009.
- 7 Appel, B. R., Tokiwa, Y., Haik, M. and Kothny, E. L.: Artifact particulate sulphate and nitrate  
8 formation on filter media, *Atmos. Environ.*, 18(2), 409–416, 1984.
- 9 Arguez, A. and Vose, R. S.: The Definition of the Standard WMO Climate Normal: The Key  
10 to Deriving Alternative Climate Normals, *Bull. Am. Meteorol. Soc.*, 92(6), 699–704,  
11 doi:10.1175/2010BAMS2955.1, 2011.
- 12 Bari, A., Ferraro, V., Wilson, L. R., Luttinger, D. and Husain, L.: Measurements of gaseous  
13 HONO, HNO<sub>3</sub>, SO<sub>2</sub>, HCl, NH<sub>3</sub>, particulate sulphate and PM<sub>2.5</sub> in New York, NY, *Atmos.*  
14 *Environ.*, 37(20), 2825–2835, doi:10.1016/S1352-2310(03)00199-7, 2003.
- 15 Barmpadimos, I., Keller, J., Oderbolz, D., Hueglin, C. and Prévôt, A. S. H.: One decade of  
16 parallel PM<sub>10</sub> and PM<sub>2.5</sub> measurements in  
17 Europe: trends and variability, *Atmospheric Chem. Phys. Discuss.*, 12(1), 1–43,  
18 doi:10.5194/acpd-12-1-2012, 2012.
- 19 Baum, M. M., Kiyomiya, E. S., Kumar, S., Lappas, A. M., Kapinus, V. A. and Lord, H. C.:  
20 Multicomponent remote sensing of vehicle exhaust by dispersive absorption spectroscopy. 2.  
21 Direct on-road ammonia measurements, *Env. Sci Technol*, 35(18), 3735–3741,  
22 doi:10.1021/es002046y, 2001.
- 23 Bond, T. C. and Bergstrom, R. W.: Light Absorption by Carbonaceous Particles: An  
24 Investigative Review, *Aerosol Sci. Technol.*, 40(1), 27–67, doi:10.1080/02786820500421521,  
25 2006.
- 26 Bressi, M., Sciare, J., Ghersi, V., Bonnaire, N., Nicolas, J. B., Petit, J.-E., Moukhtar, S.,  
27 Rosso, A., Mihalopoulos, N. and Féron, A.: A one-year comprehensive chemical  
28 characterisation of fine aerosol (PM<sub>2.5</sub>) at urban, suburban and rural  
29 background sites in the region of Paris (France), *Atmospheric Chem. Phys.*, 13(15), 7825–  
30 7844, doi:10.5194/acp-13-7825-2013, 2013.
- 31 Bussink, D. W., Harper, L. A. and Corré, W. J.: Ammonia Transport in a Temperate  
32 Grassland: II. Diurnal Fluctuations in Response to Weather and Management Conditions,  
33 *Agron J*, 88(4), 621–626, 1996.
- 34 Cavalli, F., Viana, M., Yttri, K. E., Genberg, J. and Putaud, J.-P.: Toward a standardised  
35 thermal-optical protocol for measuring atmospheric organic and elemental carbon: the  
36 EUSAAR protocol, *Atmospheric Meas. Tech.*, 3, 79–89, doi:10.5194/amt-3-79-2010, 2010.
- 37 Cheng, Y., He, K. B., Duan, F. K., Zheng, M., Ma, Y. L. and Tan, J. H.: Positive sampling

- 1 artifact of carbonaceous aerosols and its influence on the thermal-optical split of OC/EC,  
2 *Atmospheric Chem. Phys.*, 9(18), 7243–7256, 2009.
- 3 Chow, J. C., Watson, J. G., Mauderly, J. L., Costa, D. L., Wyzga, R. E., Vedal, S., Hidy, G.  
4 M., Altshuler, S. L., Marrack, D., Heuss, J. M., Wolff, G. T., Pope, C. A. and Dockery, D.  
5 W.: Health Effects of Fine Particulate Air Pollution: Lines that Connect, *J. Air Waste Manag.*  
6 *Assoc.*, 56, 1368–1380, 2006.
- 7 Collaud Coen, M., Weingartner, E., Apituley, A., Ceburnis, D., Fierz-Schmidhauser, R.,  
8 Flentje, H., Henzing, J. S., Jennings, S. G., Moerman, M. and Petzold, A.: Minimizing light  
9 absorption measurement artifacts of the Aethalometer: evaluation of five correction  
10 algorithms, *Atmospheric Meas. Tech.*, 3, 457–474, 2010.
- 11 Cowen, K., Sumner, A. L., Dinhal, A., Riggs, K. and Willenberg, Z.: Environmental  
12 Technology Verification Report, Mechatronics Instruments BV AiRRmonia Ammonia  
13 Analyzer., 2004.
- 14 Crippa, M., Canonaco, F., Slowik, J. G., El Haddad, I., DeCarlo, P. F., Mohr, C., Heringa, M.  
15 F., Chirico, R., Marchand, N., Temime-Roussel, B., Abidi, E., Poulain, L., Wiedensohler, A.,  
16 Baltensperger, U. and Prevot, A. S. H.: Primary and secondary organic aerosol origin by  
17 combined gas-particle phase source apportionment, *Atmos Chem Phys Discuss*, 13, 8537–  
18 8583, 2013a.
- 19 Crippa, M., DeCarlo, P. F., Slowik, J. G., Mohr, C., Heringa, M. F., Chirico, R., Poulain, L.,  
20 Freutel, F., Sciare, J., Cozic, J., Di Marco, C. F., Elsasser, M., Nicolas, J. B., Marchand, N.,  
21 Abidi, E., Wiedensohler, A., Drewnick, F., Schneider, J., Borrmann, S., Nemitz, E.,  
22 Zimmermann, R., Jaffrezo, J.-L., Prévôt, A. S. H. and Baltensperger, U.: Wintertime aerosol  
23 chemical composition and source apportionment of the organic fraction in the metropolitan  
24 area of Paris, *Atmospheric Chem. Phys.*, 13(2), 961–981, doi:10.5194/acp-13-961-2013,  
25 2013b.
- 26 Dall’Osto, M., Ovadnevaite, J., Ceburnis, D., Martin, D., Healy, R. M., O’Connor, I. P.,  
27 Kourtchev, I., Sodeau, J. R., Wenger, J. C. and O’Dowd, C.: Characterization of urban aerosol  
28 in Cork city (Ireland) using aerosol mass spectrometry, *Atmospheric Chem. Phys.*, 13(9),  
29 4997–5015, doi:10.5194/acp-13-4997-2013, 2013.
- 30 Draxler, R.: Hysplit4 User’s Guide. [online] Available from:  
31 <http://www.arl.noaa.gov/documents/reports/arl-230.pdf> (Accessed 14 May 2014), 1999.
- 32 Drinovec, L., Mocnik, G., Zotter, P., Prevot, A. S. H., Ruckstuhl, C., Coz Diego, E.,  
33 Rupakheti, M., Sciare, J., Mueller, T., Wiedensohler, A. T. and Hansen, A. D. A.: The “Dual-  
34 Spot” Aethalometer: improved measurement of Aerosol Black Carbon with real-time loading  
35 compensation, *Atmos Meas Tech Discuss*, 2014.
- 36 Edgerton, E. S., Saylor, R. D., Hartsell, B. E., Jansen, J. J. and Alan Hansen, D.: Ammonia  
37 and ammonium measurements from the southeastern United States, *Atmos. Environ.*, 41(16),  
38 3339–3351, doi:10.1016/j.atmosenv.2006.12.034, 2007.



- 1 Favez, O., Cachier, H., Sciare, J., Sarda-estève, R. and Martinon, L.: Evidence for a  
2 significant contribution of wood burning aerosols to PM<sub>2.5</sub> during the winter season in Paris,  
3 France, *Atmos. Environ.*, 43, 3640–3644, 2009.
- 4 Favez, O., El Haddad, I., Piot, C., Boréave, A., Abidi, E., Marchand, N., Jaffrezo, J. L.,  
5 Besombes, J. L., Personnaz, M. B., Sciare, J., Wortham, H., George, C. and D’anna, B.: Inter-  
6 comparison of source apportionment models for the estimation of wood burning aerosols  
7 during wintertime in an Alpine city (Grenoble, France), *Atmos Chem Phys*, 10, 5295–5314,  
8 doi:10.5194/acp-10-5295-2010, 2010.
- 9 Freutel, F., Schneider, J., Drewnick, F., von der Weiden-Reinmüller, S.-L., Crippa, M.,  
10 Prévôt, A. S. H., Baltensperger, U., Poulain, L., Wiedensohler, A., Sciare, J., Sarda-Estève,  
11 R., Burkhardt, J. F., Eckhardt, S., Stohl, A., Gros, V., Colomb, A., Michoud, V., Doussin, J. F.,  
12 Borbon, A., Haeffelin, M., Morille, Y., Beekmann, M. and Borrmann, S.: Aerosol particle  
13 measurements at three stationary sites in the megacity of Paris during summer 2009:  
14 meteorology and air mass origin dominate aerosol particle composition and size distribution,  
15 *Atmospheric Chem. Phys.*, 13(2), 933–959, doi:10.5194/acp-13-933-2013, 2013.
- 16 Fröhlich, R., Crenn, V., Setyan, A., Belis, C. A., Canonaco, F., Favez, O., Riffault, V.,  
17 Slowik, J. G., Aas, W., Aijälä, M., Alastuey, A., Artiñano, B., Bonnaire, N., Bozzetti, C.,  
18 Bressi, M., Carbone, C., Coz, E., Croteau, P. L., Cubison, M. J., Esser-Gietl, J. K., Green, D.  
19 C., Gros, V., Heikkinen, L., Herrmann, H., Jayne, J. T., Lunder, C. R., Minguillón, M. C.,  
20 Močnik, G., O’Dowd, C. D., Ovadnevaite, J., Petralia, E., Poulain, L., Priestman, M., Ripoll,  
21 A., Sarda-Estève, R., Wiedensohler, A., Baltensperger, U., Sciare, J. and Prévôt, A. S. H.:  
22 ACTRIS ACSM intercomparison – Part 2: Intercomparison of ME-2 organic source  
23 apportionment results from 15 individual, co-located aerosol mass spectrometers,  
24 *Atmospheric Meas. Tech. Discuss.*, 8(2), 1559–1613, doi:10.5194/amtd-8-1559-2015, 2015.
- 25 Grover, B. D.: Measurement of total PM<sub>2.5</sub> mass (nonvolatile plus semivolatile) with the  
26 Filter Dynamic Measurement System tapered element oscillating microbalance monitor, *J.*  
27 *Geophys. Res.*, 110(D7), doi:10.1029/2004JD004995, 2005.
- 28 Haeffelin, M., Barthès, L., Bock, O., Boitel, C., Bony, S., Bouniol, D., Chepfer, H., Chiriaco,  
29 M., Cuesta, J. and Delanoë, J.: SIRTA, a ground-based atmospheric observatory for cloud and  
30 aerosol research, *Ann. Geophys.*, 253–275, 2005.
- 31 Henry, R., Norris, G. A., Vedantham, R. and Turner, J. R.: Source Region Identification  
32 Using Kernel Smoothing, *Environ. Sci. Technol.*, 43(11), 4090–4097,  
33 doi:10.1021/es8011723, 2009.
- 34 IARC: Outdoor air pollution a leading environmental cause of cancer deaths, press release  
35 n°221,, 2013.
- 36 Janssen, N. A., Hoek, G., Simic-Lawson, M., Fischer, P., van Bree, L., ten Brink, H., Keuken,  
37 M., Atkinson, R. W., Anderson, H. R., Brunekreef, B. and others: Black carbon as an  
38 additional indicator of the adverse health effects of airborne particles compared with PM<sub>10</sub>  
39 and PM<sub>2.5</sub>, *Env. Health Perspect*, 119(12), 1691–1699, 2011.

- 1 Jayne, J. T., Leard, D. C., Zhang, X., Davidovits, P., Smith, K. S., Kolb, C. E. and Worsnop,  
2 D. R.: Development of an Aerosol Mass Spectrometer for Size and Composition Analysis of  
3 Submicron Particles, *Aerosol Sci. Technol.*, 33, 49–70, 2000.
- 4 Jimenez, J. L., Canagaratna, M. R., Donahue, N. M., Prevot, A. S. H., Zhang, Q., Kroll, J. H.,  
5 DeCarlo, P. F., Allan, J. D., Coe, H., Ng, N. L., Aiken, A. C., Docherty, K. S., Ulbrich, I. M.,  
6 Grieshop, A. P., Robinson, A. L., Duplissy, J., Smith, J. D., Wilson, K. R., Lanz, V. A.,  
7 Hueglin, C., Sun, Y. L., Tian, J., Laaksonen, A., Raatikainen, T., Rautiainen, J., Vaattovaara,  
8 P., Ehn, M., Kulmala, M., Tomlinson, J. M., Collins, D. R., Cubison, M. J., Dunlea, E. J.,  
9 Huffman, J. A., Onasch, T. B., Alfarra, M. R., Williams, P. I., Bower, K., Kondo, Y.,  
10 Schneider, J., Drewnick, F., Borrmann, S., Weimer, S., Demerjian, K., Salcedo, D., Cottrell,  
11 L., Griffin, R., Takami, A., Miyoshi, T., Hatakeyama, S., Shimono, A., Sun, J. Y., Zhang, Y.  
12 M., Dzepina, K., Kimmel, J. R., Sueper, D., Jayne, J. T., Herndon, S. C., Trimborn, A. M.,  
13 Williams, L. R., Wood, E. C., Middlebrook, A. M., Kolb, C. E., Baltensperger, U. and  
14 Worsnop, D. R.: Evolution of Organic Aerosols in the Atmosphere, *Science*, 326(5959),  
15 1525–1529, doi:10.1126/science.1180353, 2009.
- 16 Kai, Z., Yuesi, W., Tianxue, W., Yousef, M. and Frank, M.: Properties of nitrate, sulphate and  
17 ammonium in typical polluted atmospheric aerosols (PM10) in Beijing, *Atmospheric Res.*,  
18 84(1), 67–77, doi:10.1016/j.atmosres.2006.05.004, 2007.
- 19 Lack, D. A., Cappa, C. D., Covert, D. S., Baynard, T., Massoli, P., Sierau, B., Bates, T. S.,  
20 Quinn, P. K., Lovejoy, E. R. and Ravishankara, A. R.: Bias in Filter-Based Aerosol Light  
21 Absorption Measurements Due to Organic Aerosol Loading: Evidence from Ambient  
22 Measurements, *Aerosol Sci. Technol.*, 42(12), 1033–1041, doi:10.1080/02786820802389277,  
23 2008.
- 24 Lin, Y., Cheng, M., Ting, W. and Yeh, C.: Characteristics of gaseous HNO<sub>2</sub>, HNO<sub>3</sub>, NH<sub>3</sub>  
25 and particulate ammonium nitrate in an urban city of Central Taiwan, *Atmos. Environ.*,  
26 40(25), 4725–4733, doi:10.1016/j.atmosenv.2006.04.037, 2006.
- 27 Middlebrook, A. M., Bahreini, R., Jimenez, J. L. and Canagaratna, M. R.: Evaluation of  
28 Composition-Dependent Collection Efficiencies for the Aerodyne Aerosol Mass Spectrometer  
29 using Field Data, *Aerosol Sci. Technol.*, 46(3), 258–271,  
30 doi:10.1080/02786826.2011.620041, 2012.
- 31 Ng, N. L., Herndon, S. C., Trimborn, A., Canagaratna, M. R., Croteau, P. L., Onasch, T. B.,  
32 Sueper, D., Worsnop, D. R., Zhang, Q. and Sun, Y. L.: An aerosol chemical speciation  
33 monitor (ACSM) for routine monitoring of the composition and mass concentrations of  
34 ambient aerosol, *Aerosol Sci. Technol.*, 45(7), 780–794, 2011.
- 35 Nussbaumer, T., Czasch, C., Klippel, N., Johansson, L. and Tullin, C.: Particulate emissions  
36 from biomass combustion in IEA countries, [online] Available from: [http://www.vbt.uni-  
37 karlsruhe.de/index.pl/themen/mahe\\_wirbel/literatur/Wood-Single-  
38 Aspects/Emissions/Partikulate-Emissions-from-Biomass-Combustion-in-IEA-  
39 Countries\\_Nussbaumer\\_IEA\\_2008.pdf](http://www.vbt.uni-karlsruhe.de/index.pl/themen/mahe_wirbel/literatur/Wood-Single-Aspects/Emissions/Partikulate-Emissions-from-Biomass-Combustion-in-IEA-Countries_Nussbaumer_IEA_2008.pdf) (Accessed 11 June 2014), 2008.

- 1 Olson, D. A., Vedantham, R., Norris, G. A., Brown, S. G. and Roberts, P.: Determining  
2 source impacts near roadways using wind regression and organic source markers, *Atmos.*  
3 *Environ.*, 47, 261–268, doi:10.1016/j.atmosenv.2011.11.003, 2012.
- 4 Pal, S., Haeffelin, M. and Batchvarova, E.: Exploring a geophysical process-based attribution  
5 technique for the determination of the atmospheric boundary layer depth using aerosol lidar  
6 and near-surface meteorological measurements: NEW ATTRIBUTION LIDAR-DERIVED  
7 ABL DEPTH, *J. Geophys. Res. Atmospheres*, 118(16), 9277–9295, doi:10.1002/jgrd.50710,  
8 2013.
- 9 Pancras, J. P., Vedantham, R., Landis, M. S., Norris, G. A. and Ondov, J. M.: Application of  
10 EPA Unmix and Nonparametric Wind Regression on High Time Resolution Trace Elements  
11 and Speciated Mercury in Tampa, Florida Aerosol, *Environ. Sci. Technol.*, 45(8), 3511–3518,  
12 doi:10.1021/es103400h, 2011.
- 13 Pandolfi, M., Amato, F., Reche, C., Alastuey, A., Otjes, R. P., Blom, M. J. and Querol, X.:  
14 Summer ammonia measurements in a densely populated Mediterranean city, *Atmospheric*  
15 *Chem. Phys.*, 12(16), 7557–7575, doi:10.5194/acp-12-7557-2012, 2012.
- 16 Pathak, R., Yao, X. and Chan, C.: Sampling artifacts of acidity and ionic species in PM<sub>2.5</sub>,  
17 *Environ. Sci. Technol.*, 38(1), 254–259, doi:10.1021/es0342244, 2004.
- 18 Petit, J.-E., Favez, O., Sciare, J., Canonaco, F., Croteau, P., Močnik, G., Jayne, J., Worsnop,  
19 D. and Leoz-Garziandia, E.: Submicron aerosol source apportionment of wintertime pollution  
20 in Paris, France by Double Positive Matrix Factorization (PMF<sup>2</sup>)</sup> using Aerosol Chemical Speciation Monitor (ACSM) and multi-wavelength Aethalometer,  
21 *Atmospheric Chem. Phys. Discuss.*, 14(10), 14159–14199, doi:10.5194/acpd-14-14159-2014,  
22 2014.  
23
- 24 Pope, C. A. and Dockery, D. W.: Health Effects of Fine Particulate Air Pollution: Lines that  
25 Connect, *J. Air Waste Manag. Assoc.*, 56(6), 709–742,  
26 doi:10.1080/10473289.2006.10464485, 2006.
- 27 Putaud, J.-P., Raes, F., Van Dingenen, R., Brüggemann, E., Facchini, M.-C., Decesari, S.,  
28 Fuzzi, S., Gehrig, R., Hüglin, C., Laj, P., Lorbeer, G., Maenhaut, W., Mihalopoulos, N.,  
29 Müller, K., Querol, X., Rodriguez, S., Schneider, J., Spindler, G., Brink, H. ten, Tørseth, K.  
30 and Wiedensohler, A.: A European aerosol phenomenology—2: chemical characteristics of  
31 particulate matter at kerbside, urban, rural and background sites in Europe, *Atmos. Environ.*,  
32 38(16), 2579–2595, doi:10.1016/j.atmosenv.2004.01.041, 2004.
- 33 Ramgolam, K., Favez, O., Cachier, H., Gaudichet, A., Marano, F., Martinon, L. and Baeza-  
34 Squiban, A.: Size-partitioning of an urban aerosol to identify particle determinants involved in  
35 the proinflammatory response induced in airway epithelial cells, *Part. Fibre Toxicol.*, 6(10),  
36 doi:10.1186/1743-8977-6-10, 2009.
- 37 Rengarajan, R., Sudheer, A. K. and Sarin, M. M.: Wintertime PM<sub>2.5</sub> and PM<sub>10</sub> carbonaceous  
38 and inorganic constituents from urban site in western India, *Atmospheric Res.*, 102(4), 420–  
39 431, doi:10.1016/j.atmosres.2011.09.005, 2011.

1 Sandradewi, J., Prévôt, A. S. H., Szidat, S., Perron, N., Alfarra, M. R., Lanz, V. A.,  
2 Weingartner, E. and Baltensperger, U.: Using Aerosol Light Absorption Measurements for  
3 the Quantitative Determination of Wood Burning and Traffic Emission Contributions to  
4 Particulate Matter, *Environ. Sci. Technol.*, 42(9), 3316–3323, doi:10.1021/es702253m, 2008.

5 Saylor, R. D., Edgerton, E. S., Hartsell, B. E., Baumann, K. and Hansen, D. A.: Continuous  
6 gaseous and total ammonia measurements from the southeastern aerosol research and  
7 characterization (SEARCH) study, *Atmos. Environ.*, 44(38), 4994–5004,  
8 doi:10.1016/j.atmosenv.2010.07.055, 2010.

9 Sciare, J., d' Argouges, O., Sarda-Estève, R., Gaimoz, C., Dolgorouky, C., Bonnaire, N.,  
10 Favez, O., Bonsang, B. and Gros, V.: Large contribution of water-insoluble secondary organic  
11 aerosols in the region of Paris (France) during wintertime, *J. Geophys. Res. Atmospheres*,  
12 116(D22), n/a–n/a, doi:10.1029/2011JD015756, 2011.

13 Sciare, J., d' Argouges, O., Zhang, Q. J., Sarda-Estève, R., Gaimoz, C., Gros, V., Beekmann,  
14 M. and Sanchez, O.: Comparison between simulated and observed chemical composition of  
15 fine aerosols in Paris (France) during springtime: contribution of regional versus continental  
16 emissions, *Atmospheric Chem. Phys.*, 10(24), 11987–12004, doi:10.5194/acp-10-11987-  
17 2010, 2010.

18 Sciare, J., Sarda-estève, R., Favez, O., Cachier, H., Aymoz, G. and Laj, P.: Nighttime  
19 residential wood burning evidenced from an indirect method for estimating real-time  
20 concentration of particulate organic matter (POM), *Atmos. Environ.*, 42, 2158–2172, 2008.

21 Takegawa, N., Miyazaki, Y., Kondo, Y., Komazaki, Y., Miyakawa, T., Jimenez, J. L., Jayne,  
22 J. T., Worsnop, D. R., Allan, J. D. and Weber, R. J.: Characterization of an Aerodyne Aerosol  
23 Mass Spectrometer (AMS): Intercomparison with Other Aerosol Instruments, *Aerosol Sci.*  
24 *Technol.*, 39(8), 760–770, doi:10.1080/02786820500243404, 2005.

25 Turpin, B. J., Huntzicker, J. J. and Hering, S. V.: Investigation of organic aerosol sampling  
26 artifacts in the Los Angeles Basin, *Atmos. Environ.*, 28(19), 3061–3071, 1994.

27 Waked, A., Favez, O., Alleman, L. Y., Piot, C., Petit, J.-E., Delaunay, T., Verlinden, E.,  
28 Golly, B., Besombes, J.-L., Jaffrezo, J.-L. and Leoz-Garziandia, E.: Source apportionment of  
29 PM<sub>10</sub> in a north-western Europe regional urban background site  
30 (Lens, France) using positive matrix factorization and including primary biogenic emissions,  
31 *Atmospheric Chem. Phys.*, 14(7), 3325–3346, doi:10.5194/acp-14-3325-2014, 2014.

32 Weingartner, E., Saathoff, H., Schnaiter, M., Streit, N., Bitnar, B. and Baltensperger, U.:  
33 Absorption of light by soot particles: determination of the absorption coefficient by means of  
34 aethalometers, *J. Aerosol Sci.*, 34, 1445–1463, 2003.

35 Yiou, P. and Cattiaux, J.: Contribution of Atmospheric circulation to wet North European  
36 summer precipitation of 2012, *Am. Meteorol. Soc.* [online] Available from:  
37 [http://docs.house.gov/meetings/IF/IF03/20130918/101308/HHRG-113-IF03-20130918-](http://docs.house.gov/meetings/IF/IF03/20130918/101308/HHRG-113-IF03-20130918-SD011.pdf)  
38 [SD011.pdf](http://docs.house.gov/meetings/IF/IF03/20130918/101308/HHRG-113-IF03-20130918-SD011.pdf) (Accessed 14 May 2014), 2013.

- 1 Yu, K. ., Cheung, Y. ., Cheung, T. and Henry, R. C.: Identifying the impact of large urban  
2 airports on local air quality by nonparametric regression, *Atmos. Environ.*, 38(27), 4501–  
3 4507, doi:10.1016/j.atmosenv.2004.05.034, 2004.
- 4 Zechmeister-Boltenstern, S.: Training on NH<sub>3</sub> measurement by wet chemistry techniques,  
5 ACTRIS TNA Activity Report., 2010.
- 6 Zhang, Q., Jimenez, J. L., Canagaratna, M. R., Allan, J. D., Coe, H., Ulbrich, I., Alfarra, M.  
7 R., Takami, A., Middlebrook, A. M., Sun, Y. L., Dzepina, K., Dunlea, E., Docherty, K.,  
8 DeCarlo, P. F., Salcedo, D., Onasch, T., Jayne, J. T., Miyoshi, T., Shimo, A., Hatakeyama,  
9 S., Takegawa, N., Kondo, Y., Schneider, J., Drewnick, F., Borrmann, S., Weimer, S.,  
10 Demerjian, K., Williams, P., Bower, K., Bahreini, R., Cottrell, L., Griffin, R. J., Rautiainen,  
11 J., Sun, J. Y., Zhang, Y. M. and Worsnop, D. R.: Ubiquity and dominance of oxygenated  
12 species in organic aerosols in anthropogenically-influenced Northern Hemisphere  
13 midlatitudes, *Geophys. Res. Lett.*, 34(13), doi:10.1029/2007GL029979, 2007.
- 14 Zhang, Q., Stanier, C. O., Canagaratna, M. R., Jayne, J. T., Worsnop, D. R., Pandis, S. N. and  
15 Jimenez, J. L.: Insights into the Chemistry of New Particle Formation and Growth Events in  
16 Pittsburgh Based on Aerosol Mass Spectrometry, *Environ. Sci. Technol.*, 38(18), 4797–4809,  
17 doi:10.1021/es035417u, 2004.

18

19 |

1 Table 1. Response factors obtained through IE calibrations from June 2011 to May 2013

Date	Response Factor	RIE <sub>NH4</sub>	RIE <sub>SO4</sub>
16/11/2011	2.31 10 <sup>-11</sup>	6	-
09/10/2012	2.98 10 <sup>-11</sup>	4.8	-
15/05/2013	2.84 10 <sup>-11</sup>	6.84	1.25
<b>Average</b>	<b>2.72 10<sup>-11</sup></b>	<b>5.88</b>	-
<b>Standard deviation</b>	<b>13%</b>	<b>17%</b>	-

2

3

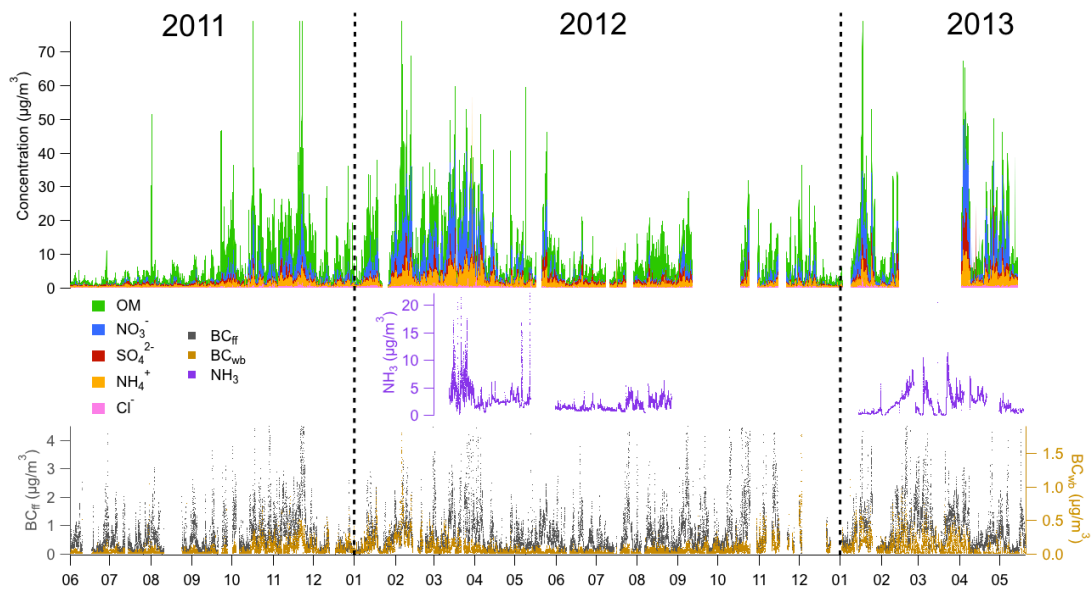
4

1 Table 2. Essential parameters describing the 8 pollution episodes, such as the start and end date, average temperature and relative humidity,  
 2 fraction dominating the chemical composition (SIA stands for Secondary Inorganic Aerosols), BC-to-SO<sub>4</sub> ratio and main geographical  
 3 contribution

Episode #	Start –end date	Temp. (°C)	RH (%)	Chemical Composition	BC/SO <sub>4</sub>	Geographical contribution
1	19/11/2011 - 24/11/2011	8.5	93	OM	3.56	Regional
2	05/02/2012 - 13/02/2012	-4.7	71	OM then SIA	0.91	Strong local, then regional and advected
3	29/02/2012 - 03/03/2012	8.2	95	SIA	1.12	Strong regional, low advected
4	12/03/2012 - 17/03/2012	10.7	78	SIA	0.95	Advected and regional
5	23/03/2012 - 26/03/2012	15	48	SIA	2.37	Strong advected, low regional
6	28/03/2012 - 31/03/2012	12.3	62	SIA	1.42	Strong advected and regional
7	16/01/2012 - 21/01/2012	-3	93	OM & SIA	0.72	Strong regional and advected
8	01/04/2013 - 08/04/2013	4.2	64	SIA	0.12	Advected

4

1

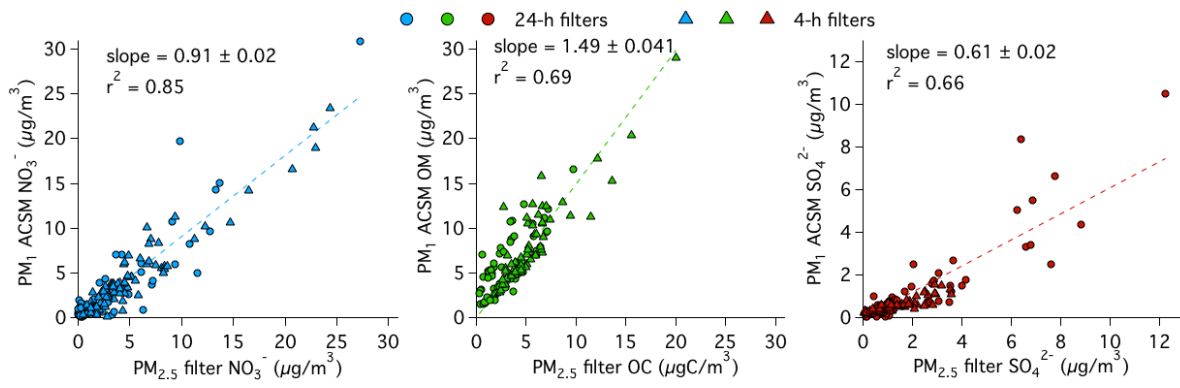


2

3 Figure 1: Time series of the major 30-min non-refractory (top, concentrations are aggregated)  
4 and 5-min refractory (bottom, concentrations are dissociated) PM<sub>1</sub> chemical constituents, and  
5 5-min ammonia at SIRT from June 2011 to May 2013. The two large data gaps in October  
6 2012 and March 2013 correspond to two field intensive campaigns during which the ACSM  
7 was deployed elsewhere.

8

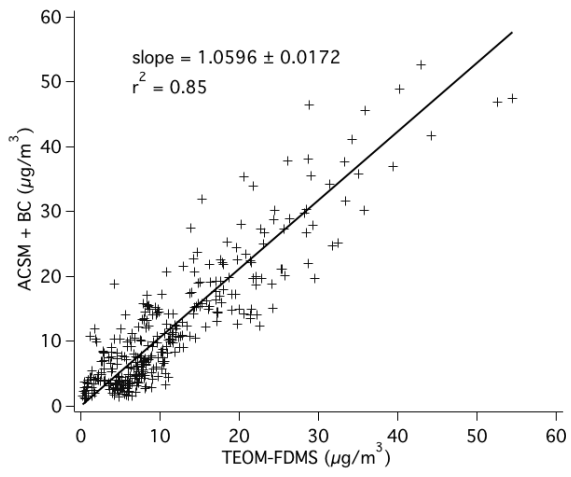




1

2 Figure 2: Scatter plot of chemically-specified ACSM measurements versus filter analyses for  
 3 nitrate, organic matter (compared to OC filter-based measurements) and sulphate.

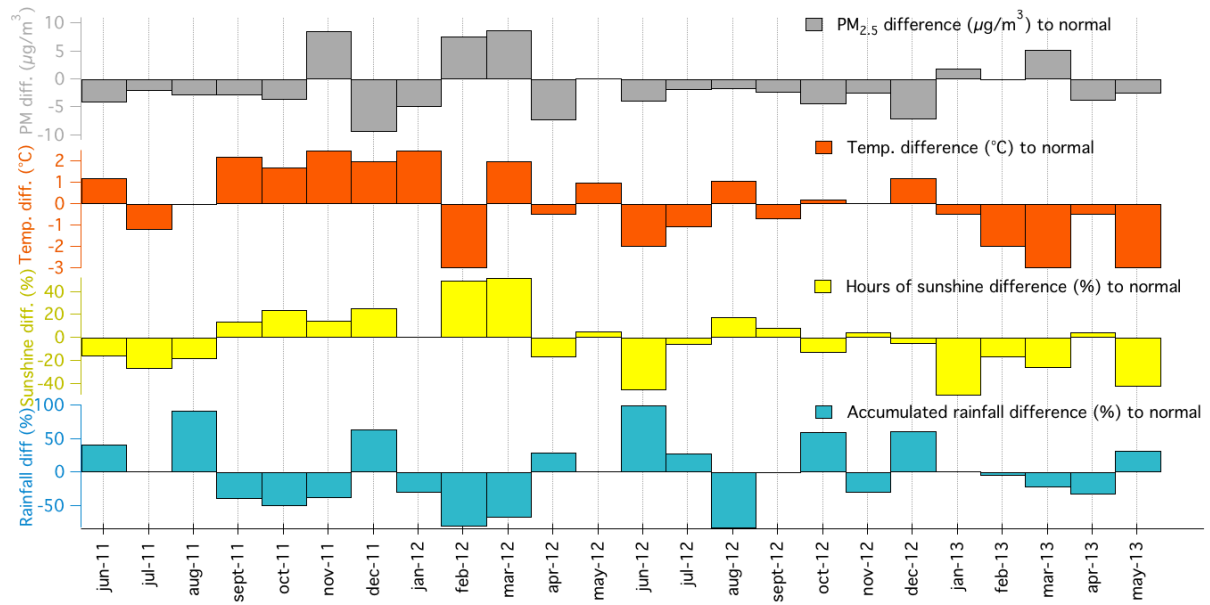
4



1

2 Figure 3: Mass closure exercise between daily averaged reconstructed  $\text{PM}_{10}$  (ACSM + BC)  
3 and measured  $\text{PM}_{10}$  by TEOM-FDMS.

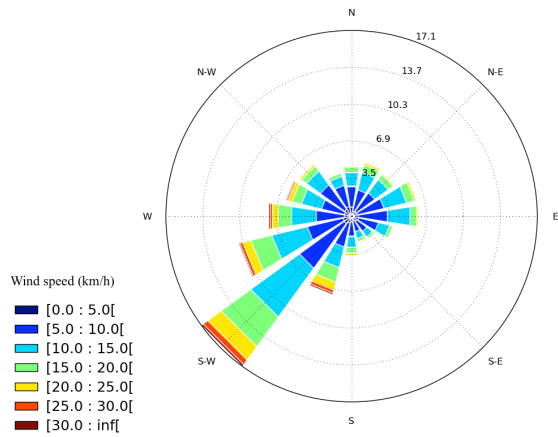
4



1

2 Figure 4: Comparison between observed and average PM<sub>2.5</sub>, temperature, hours of sunshine  
 3 and accumulated rainfall in the region of Paris.

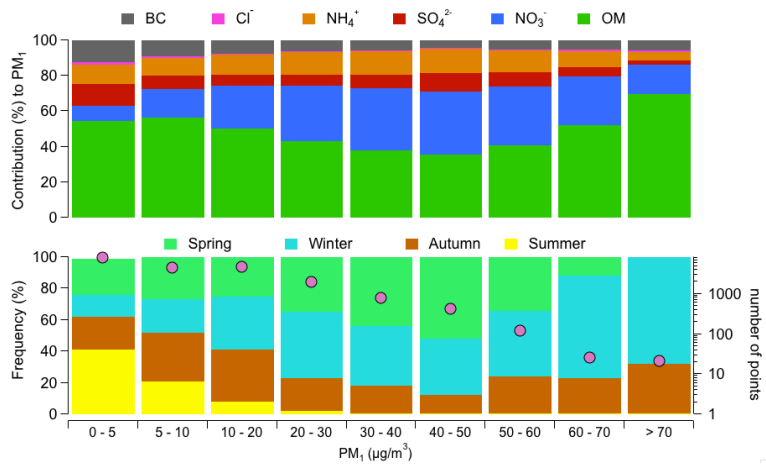
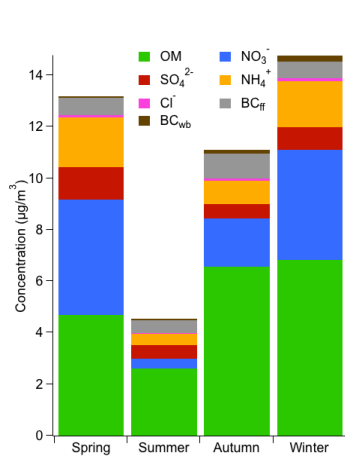
4



1

2 Figure 5: Average wind rose during Jun. 2011 and Jun. 2013, the radial axis represents the  
 3 wind occurrence (in %).

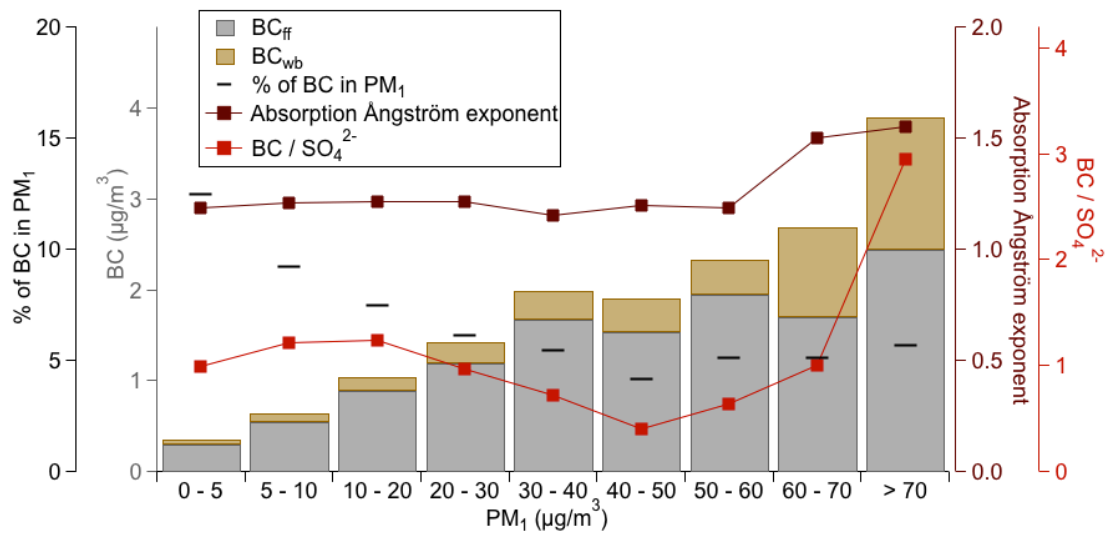
4



1

2 Figure 6: a) PM<sub>1</sub> chemical composition for different mass classes (top), with the seasonal  
 3 occurrence frequency and number of points in each bin (bottom) b) seasonal PM<sub>1</sub> chemical  
 4 composition.

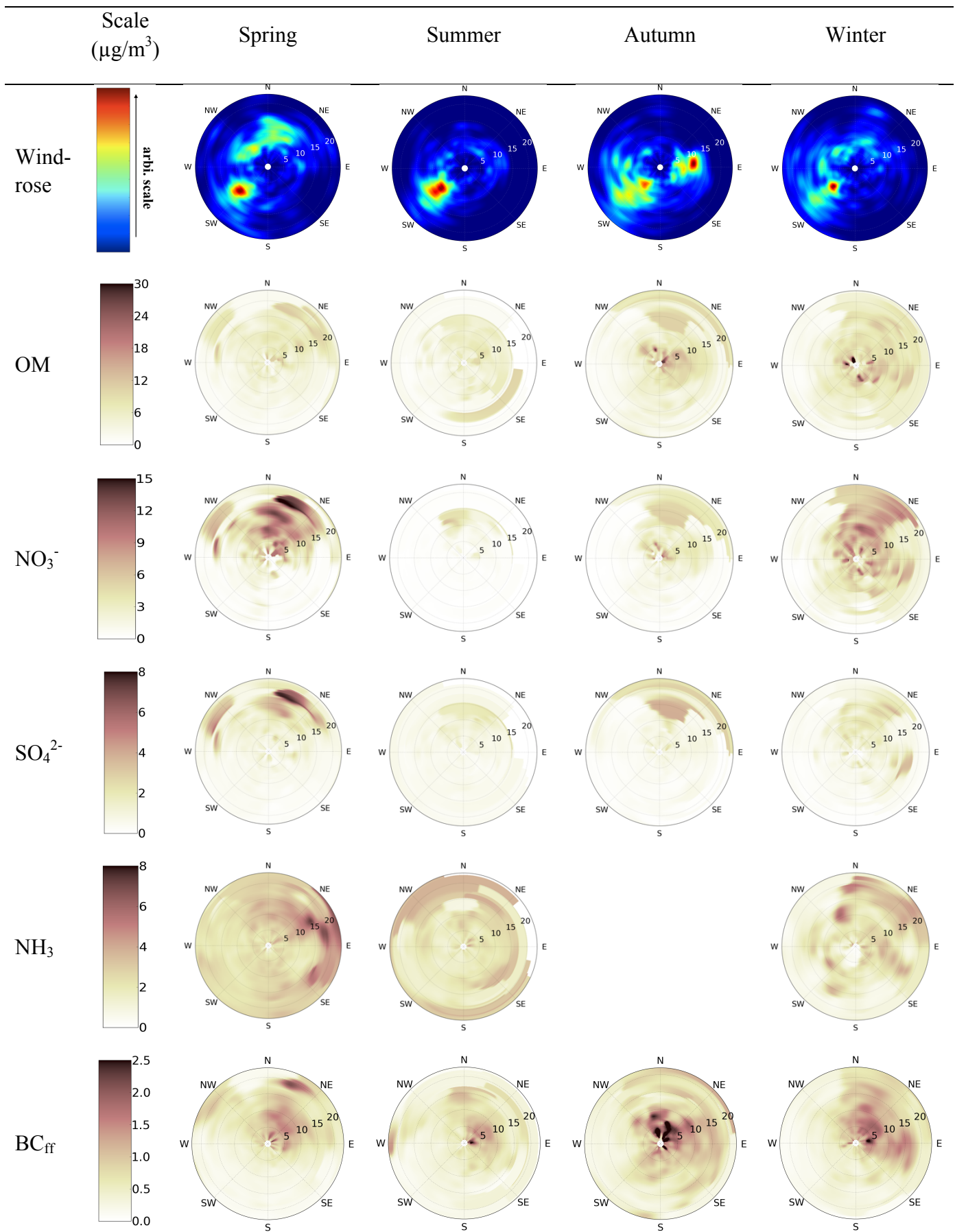
5

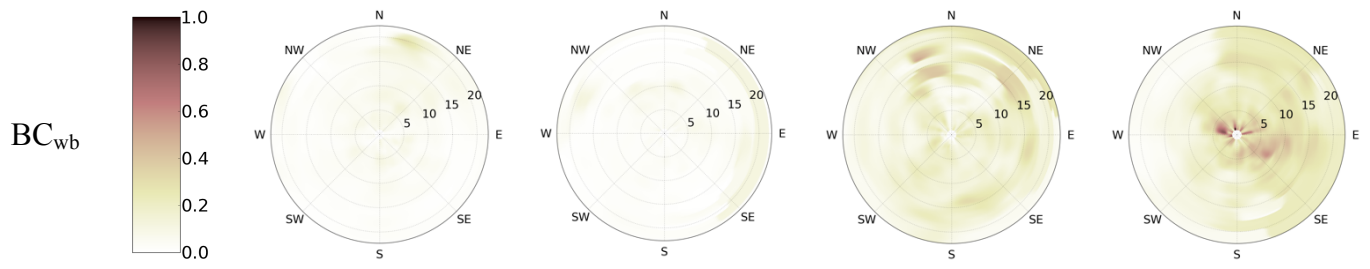


1

2 Figure 7: Source contribution to BC, absorption Ångström exponent, BC-SO<sub>4</sub> ratio (ACSM  
 3 sulphate), and contribution of BC to PM<sub>1</sub>, depending on PM<sub>1</sub> mass.

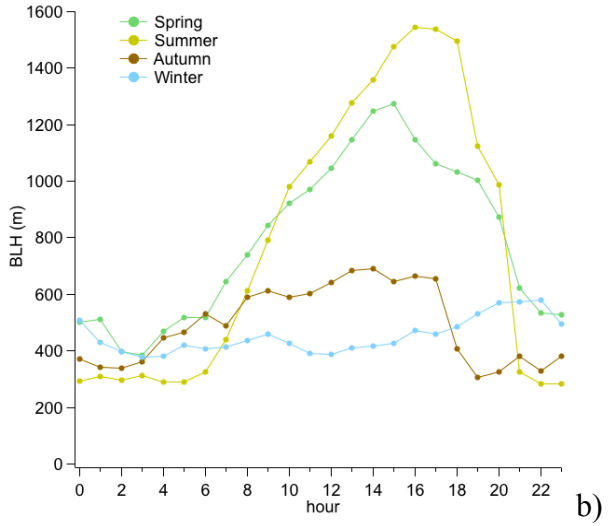
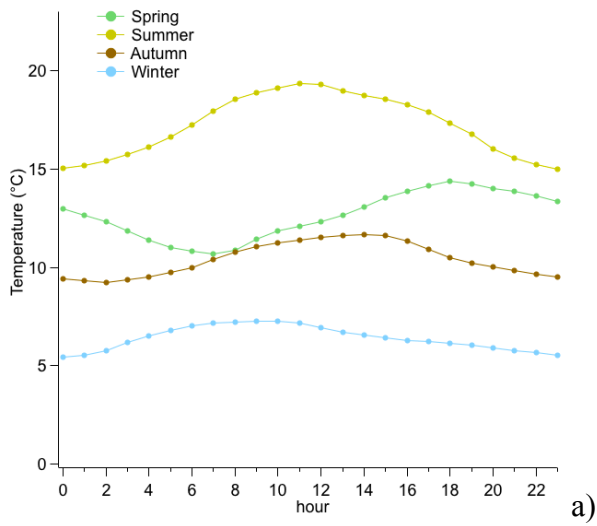
4





- 
- 1 Figure 8: Seasonal NWR plots for the major components of  $PM_{10}$  and gaseous ammonia.
  - 2 Radial and tangential axes represent the wind direction and speed (km/h), respectively.
  - 3

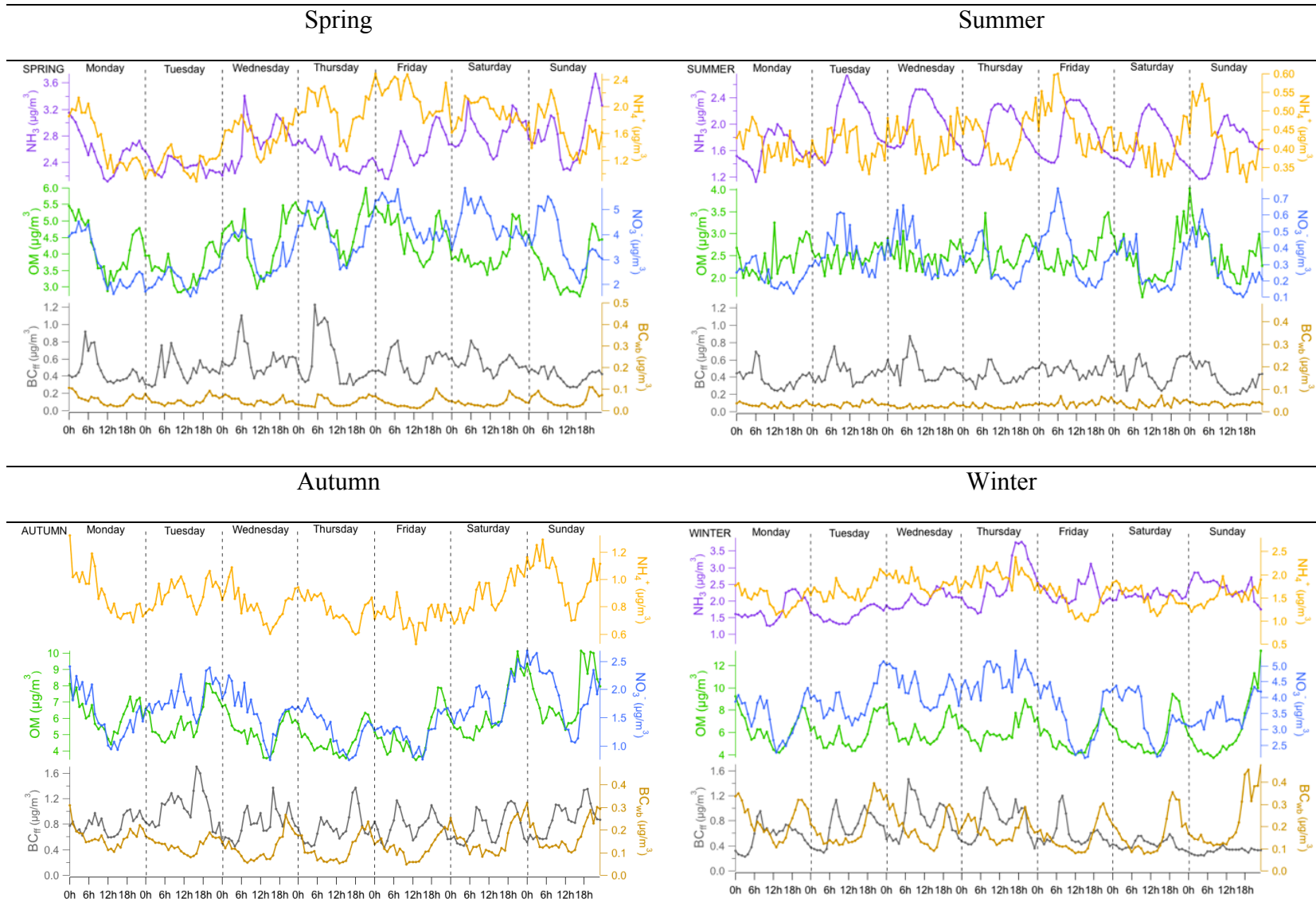




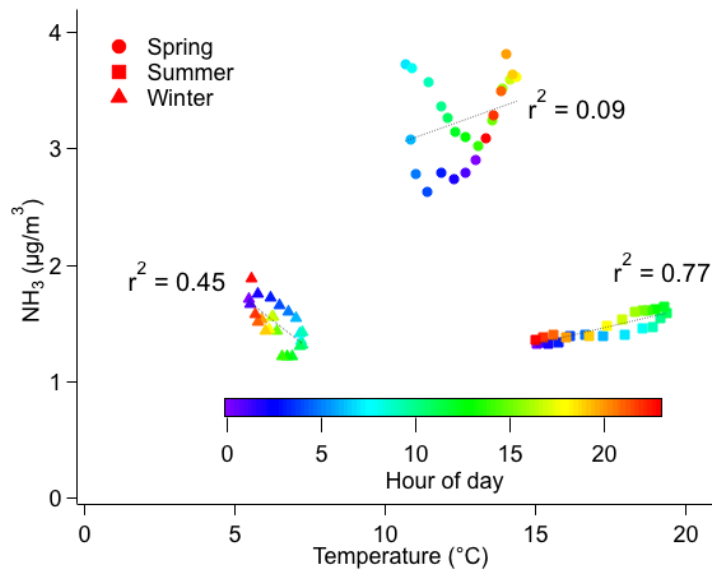
1

2 Figure 9: Average diurnal variations by seasons of temperature (a) and BLH (b)

3



1 Figure 10: Seasonal weekly diurnal variations of OM (green),  $\text{NO}_3^-$  (blue),  $\text{NH}_4^+$  (dark yellow),  $\text{NH}_3$  (purple),  $\text{BC}_{\text{ff}}$  (black) and  $\text{BC}_{\text{wb}}$  (brown)

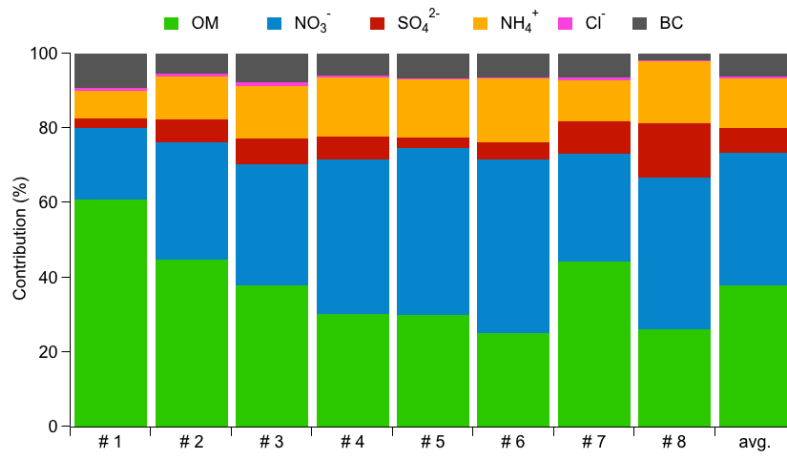


1

2 Figure 11: Correlation between ammonia and temperature in Spring (circles), Summer  
 3 (squares) and Winter (triangles) coloured as a function of the hour of day.

4

1



2

3 Figure 12: PM<sub>1</sub> chemical composition of the 8 pollution episodes

BC/SO<sub>4</sub><sup>2-</sup>

Backtrajectories and altitudes

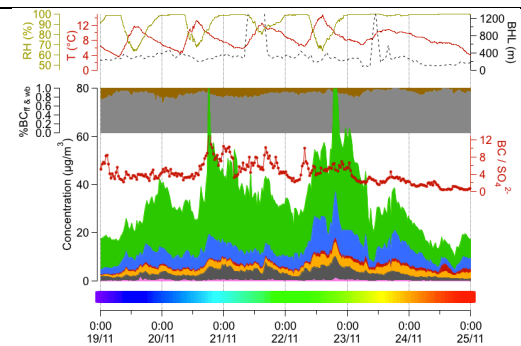
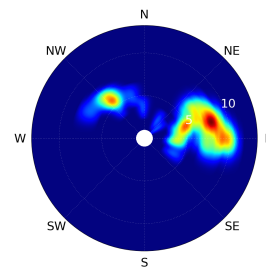
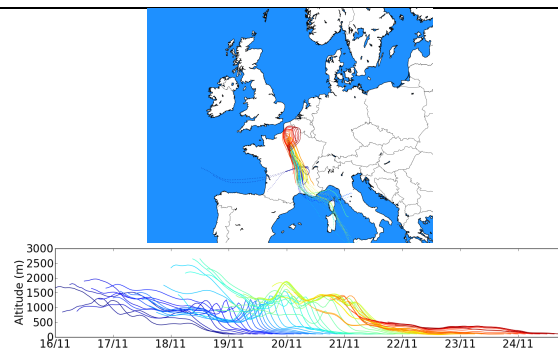
Wind rose

Chemical composition & meteo. param.

#1

19/11/2011 – 24/11/2011

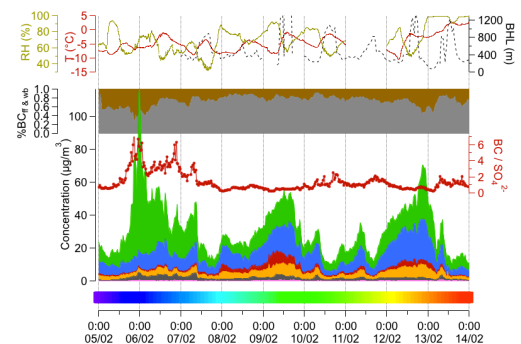
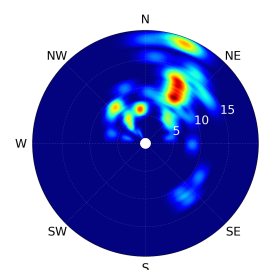
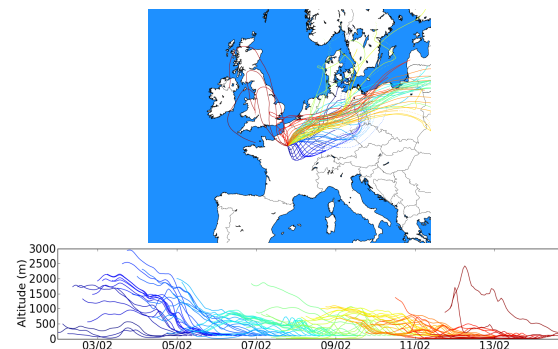
3.56



#2

05/02/2012 – 14/02/2012

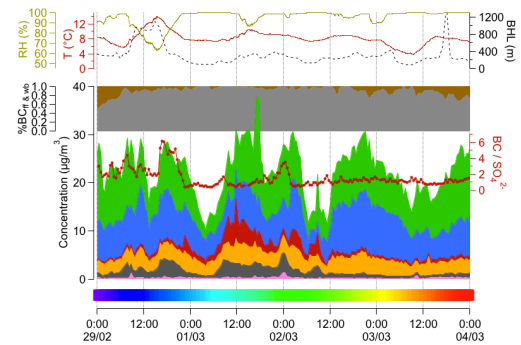
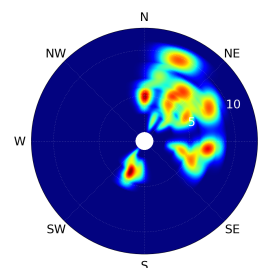
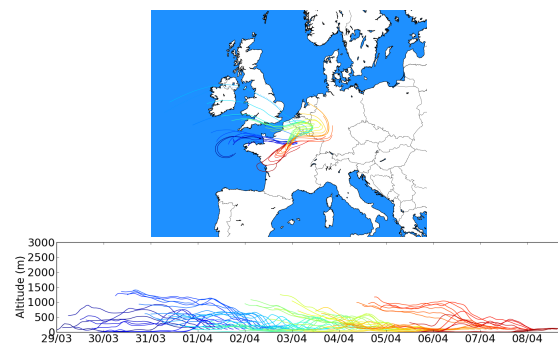
0.91



#3

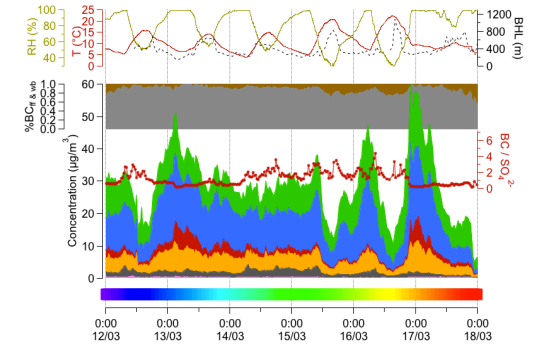
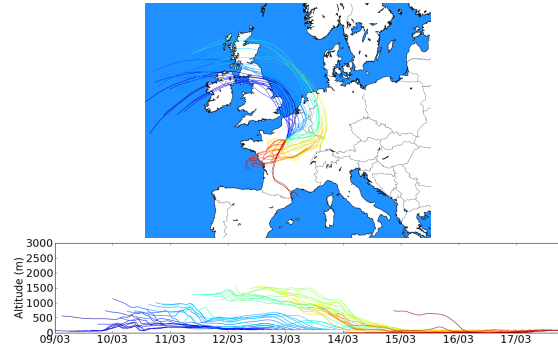
29/02/2012 – 04/03/2012

1.12



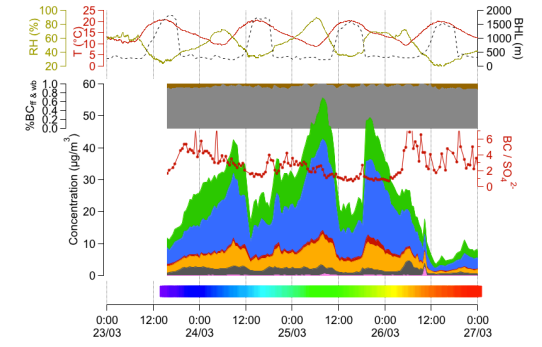
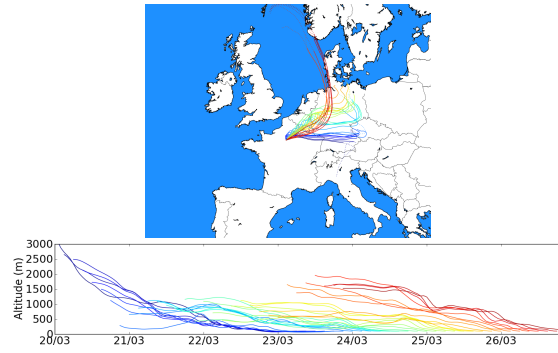
#4  
12/03/2012 – 18/03/2012

0.95



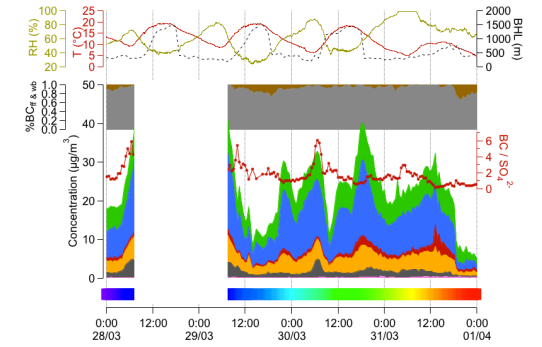
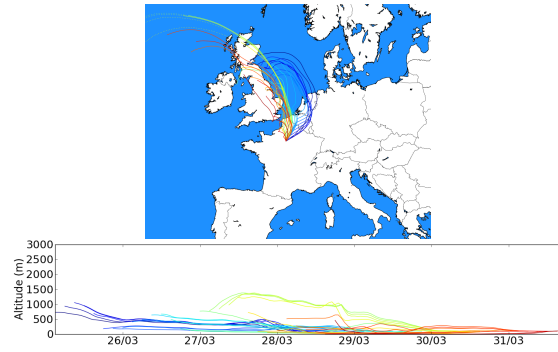
#5  
23/03/2012 – 26/03/2012

2.37



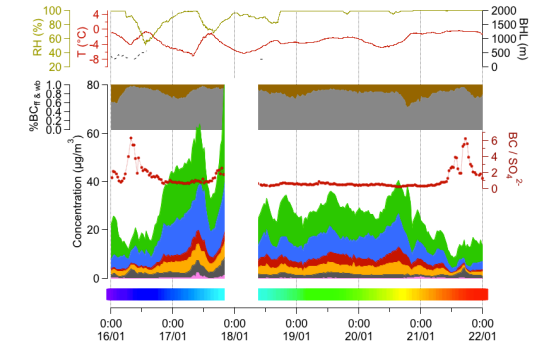
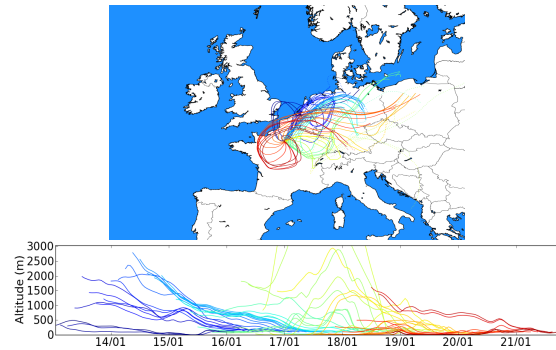
#6  
28/03/2012 – 01/04/2012

1.42



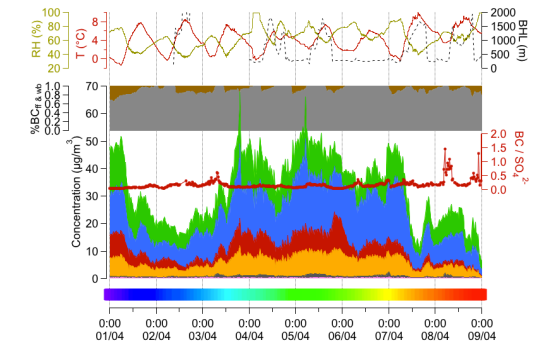
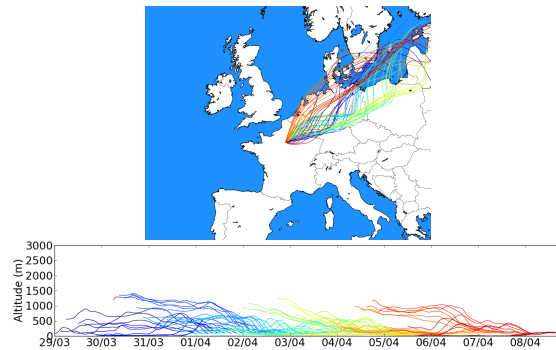
#7  
16/01/2013 – 21/01/2013

0.72



#8  
01/04/2013 – 09/04/2013

0.12



1 Figure 13: Illustration of meteorological conditions and chemical composition during the 8 pollution episodes. Left graphs represent 72h-backtrajectories  
 2 ending at Sirta at 100 m a.g.l. every 3h and their altitude; Middle graphs illustrate the wind rose (radial axis in km/h); Right graphs represent the chemical  
 3 composition, in  $\mu\text{g}/\text{m}^3$  of submicron particle (organic, nitrate, sulphate, ammonium, chloride and black carbon in green, blue, red, orange, pink and dark grey,  
 4 respectively), the contribution of traffic and wood-burning to BC, the  $\text{BC}/\text{SO}_4^{2-}$  ratio, and temperature, RH and BLH